IMPROVING DISTRIBUTION SYSTEM RELIABILITY THROUGH RISK-BASED OPTIMIZATION OF FAULT MANAGEMENT AND IMPROVED COMPUTER-BASED FAULT LOCATION

A Dissertation

by

YIMAI DONG

Submitted to the Office of Graduate and Professional Studies of
Texas A&M University
in partial fulfillment of the requirements for the degree of

DOCTOR OF PHILOSOPHY

Chair of Committee,	Mladen Kezunovic
Committee Members,	Garng Huang
	Ulisses Braga-Neto
	Erick Moreno-Centeno
Head of Department,	Chanan Singh

December 2013

Major Subject: Electrical Engineering

ABSTRACT

Utilities of distribution systems now are under the pressure of improving the reliability of power supply, not only from the urge to increase revenue, but also from requirements of their customers and the Independent Service Organization (ISO)'s regulation on power quality. Optimization in fault management tasks has the potential of improving system reliability by reducing the duration and scale of outages caused by faults through fast fault isolation and service restoration.

The research reported by this dissertation aims at improving distribution system reliability through optimized fault management. Three questions are explored and answered: 1) how to establish the cause-and-effect relationship between fault management and system reliability; 2) how can individual fault management tasks benefit from the newly emerged smart grid technologies; and 3) how to improve the overall performance of fault management under new operation condition.

Optimization of the fault management is done through minimizing a risk function representing system reliability. The improvement in system reliability is approached in following steps: 1) a risk function consists of distribution reliability indices is defined as the criterion for system reliability; 2) a new fault location method is proposed first that can accurately locate the faults with the assistance of voltage-sag-measurements from system-wide Intelligent Electronics Devices (IEDs); 3) the fault management task of field inspection is optimized using the risk function and the probability model of the true fault location established using results from fault location; 4) the decision making on the execution of during-fault service restoration is optimized through Monte Carlo

simulation; 5) the optimized fault management is utilized in processing the faults and the improvement in system reliability is assessed by reduction of costs associated with these faults.

The proposed optimization is demonstrated on a realistic distribution system. The stochastic model of faults in the system is built with consideration of normal and extreme weather conditions. Results show that the proposed optimization is capable of improving system reliability by reducing the mean and variance of outage cost calculated over the simulated years.

DEDICATION

To my husband Dr. Ce Zheng and my son Kevin.

ACKNOWLEDGEMENTS

I would like to acknowledge my committee chair, Dr. Mladen Kezunovic, and my committee members, Dr. Huang, Dr. Braga-Neto, and Dr Moreno-Centeno, for their guidance and support throughout the course of this research. I would also like to take this chance to pay my respect and appreciation to the deceased Dr. Lively, who was my committee member and was of great support.

Appreciation also goes to my friends and colleagues and the department faculty and staff for making my time at Texas A&M University a great experience. I would especially thank Dr. Chengzong Pang, Dr. Yufan Guan, Dr. Jinfeng Ren and Dr. Saeed Lotfifard for their help along the way.

Thanks also go to my parents. I wouldn't have achieved what I have done without their encouragement.

NOMENCLATURE

ASIDI	Average Service Interruption Duration Index
DA	Distribution Automation
DMS	Distribution Management System
DT	Decision Tree
FA	Feeder Automation
FL	Fault Location
IED	Intelligent Electronics Device
OMS	Outage Management System
RI	Reliability Index
SAIDI	System Average Interruption Duration Index
SG	Smart Grid
TTNF	Time To Next Fault

TABLE OF CONTENTS

Page

ABSTRACT ii

DEDICATION iv

ACKNOWLEDGEMENTS v

NOMENCLATURE vi

TABLE OF CONTENTS vii

LIST OF FIGURES x

LIST OF TABLES xii

1. INTRODUCTION 1

1.1 Problem statement 1
1.2 Unsolved issues 2
1.3 Objective of this study 2

2. SUREVEY OF PREVIOUS STUDIES 3

2.1 Overview of the application-level fault management 3
2.2 State of art on fault location 4
2.3 Optimized crew management and service restoration 4

3. PROBLEM FORMULATION 6

3.1 Introduction to fault management 6
3.2 Assistance to fault management from new smart grid technologies 8
3.3 Impact of fault management on system reliability 9
3.4 Formulation of the problem 10

4. RISK-ANALYSIS BASED OPTIMIZATION OF FAULT MANAGEMENT 12

4.1 Introduction and formulation of outage cost 12
4.2 Formulation of risk function 14
4.3 Fault management functions of interest 15
4.4 Conclusion 15

5. IMPROVED FAULT LOCATION METHOD 17

5.1 Introduction 17
5.2 Voltage measurement-based methods 17
5.3 Pereira's Algorithm [30] 18
5.4 Limitations in Pereira's Algorithm 20
5.5 Proposed fault location method 22
5.6 Conclusion 25

6. OPTIMIZED CREW DISPATCH 26

6.1 Introduction 26
6.2 Formulation of the crew dispatch optimization 27
6.3 Calculation of P_i and T_i 27
6.4 Conclusion 29

7. OPTIMIZED SERVICE RESTORATION 30

7.1 Introduction 30
7.2 Formulation of optimization problem 32
7.3 Conclusion 34

8. APPROACH TO THE ASSESSMENT OF BENEFITS 35

8.1 Introduction 35
8.2 Calculation of profit 35
8.3 Conclusion 37

9. IMPLEMENTATION OF THE PROPOSED STUDY 38

9.1 System model 38
9.2 Implementation of fault location method 39
9.3 Implementation of Monte Carlo Simulation 42
9.4 Conclusion 45

10. CASE STUDY 46

10.1 Improved fault location 46
10.2 Optimized fault management functions 54
10.3 Assessment of benefit 57
10.4 Conclusion 61

11. CONCLUSION 62

11.1 Research achievements and contributions 62
11.2 Conclusions 62
11.3 Suggestions for future work 63

REFERENCES 65

APPENDIX 71

LIST OF FIGURES

Page

Figure 1 Overview of fault management functions [14] 7

Figure 2 Distribution automation deployment 9

Figure 3 Proposed fault management process 11

Figure 4 One-line diagram of a feeder 20

Figure 5 Z_x with different R_f and $|Z_{b1}|$, $\angle Z_{b1}=60°$, $Z_{L2}\rightarrow inf.$, $Z_{L\Sigma}=500\angle 30°$ 22

Figure 6 Procedures of the proposed fault location scheme 23

Figure 7 Composition of T_i 28

Figure 8 Procedures for estimating $\Delta Risk$ 34

Figure 9 Generation of fault scenarios 36

Figure 10 Calculation of the outage time 37

Figure 11 Topology of the 13.8 kV, 134-node, overhead distribution system 39

Figure 12 Procedure of knowledge base generation 40

Figure 13 Decision Tree topology for segment identification 42

Figure 14 Computation of reliability indices using Monte Carlo simulation 44

Figure 15 Fault location errors in km with faults along the feeder 48

Figure 16 Mismatch calculated for fault at node 24, R_f=0 49

Figure 17 Output from segment identifier, with R_f=1Ω 49

Figure 18 Improvement with segment identifier 50

Figure 19 Errors under load variation (Scenario Group 8) 53

Figure 20 Reduction in fault location errors 53

Figure 21 ASIDIs calculated with different T_{SWC} 57

Figure 22 SAIDI results for original status 58

Figure 23 ASIDIs of RecS1, T_{COM}=30 min 60

LIST OF TABLES

Page

Table 1 Settings for Test Scenarios 43

Table 2 Description of Scenario Groups and Rate of Successful Segment Identification 46

Table 3 Errors in Perfect Condition 51

Table 4 Test Results from Non-Perfect Condition Scenarios 52

Table 5 Optimized Fault Location and Isolation Plan 55

Table 6 Connectivity to Adjacent Feeders 57

Table 7 Simulation Results 60

1. INTRODUCTION

1.1 Problem statement

Feeder faults are the causes of most distribution-level outages and reliability problems [1]. Time to locate and isolate a feeder fault may take a considerable portion in the total duration of the outage, due to the vast geographical coverage of the system, and a low degree of monitoring instrumentation. Time to repair may vary case by case, depending on the cause, type, time of occurrence, and other fault characteristics [2].

An Outage Management System (OMS) provides outage reports for repair crew and operators to restore the network after outages [3]. Outage information comes from different sources: Trouble Calls system, Automatic Meter Reading (AMR) system, Supervisory Control and Data Acquisition (SCADA) system, as well as Geographical Information System [4]. Fault management is a subset of OMS functionality that explicitly deals with fault location, repair and restoration of a faulted feeder [5].

Analysis of temporal trends in distribution reliability shows that installation and update of Outage Management Systems (OMS) reduce the overall duration of outages [6]. Automating fault management tasks and optimizing their execution have the potential to further enhance power system reliability and increase customer satisfaction. These require handling of the uncertainty intrinsic to fault scenarios. Therefore a risk-based optimization approach needs to be explored.

1.2 Unsolved issues

While much work has been done on computer-based fault location [7], a review of literature reveals that the optimization of fault management tasks has not been fully studied yet. The areas that remain inadequately explored include how to interpret the multiple solutions and possible errors from the estimation of fault location, and how to utilize them in the subsequent steps of crew dispatch and necessary post-fault reconfiguration.

In the meantime, the impact of fault management tasks on system reliability needs to be carefully assessed [8]. For example, utilities now assume that a fault location outcome providing the correct line segment is precise enough. Without quantitative evidence on how much the savings may be, they may not be convinced of the benefit from installing new sensors and adopting new fault location methods. It is imperative to develop a method of assessing the benefit from optimizing fault management tasks, for both performance evaluation and cost-impact analysis purposes.

1.3 Objective of this study

This dissertation focuses on the optimization of fault management tasks in the following aspects:

1) improvement in accuracy of fault location computation;

2) optimization of crew dispatch based on results from step 1;

3) streamlining of decision-making in system reconfiguration; and

4) quantifying the assessment of benefits.

2. SUREVEY OF PREVIOUS STUDIES

2.1 Overview of the application-level fault management

The use of performance-based rates with financial penalties for poor performance is a commercial incentive for utilities to better manage outages attributable to system faults [9]-[14]. In [9] various approaches for implementing Fault Detection, Isolation and Restoration (FDIR) schemes is reviewed and compared. Based on the number of intelligent controllers and the infrastructure of communication, fault management can be classified as distributed (local) fault management, where feeder faults are treated by the local intelligent controller using locally acquired data, and centralized fault management, where data from all over the system is transferred to a centralized location using a Supervisory Controlling And Data Acquisition (SCADA) system and centeralized Distribution Management System (DMS). In general, the centralized FM analyzes faults more comprehensively and allows for more complex switching scenarios. Therefore, the capacity for neighboring feeders to pickup loads from the faulted feeder is enhanced on the stage of service restoration.

[11] investigated the application-level issues associated with FM and automation schemes that helps accelerate the process of fault location and fault isolation. Discussion of possible improvement to FM is reported. Factors to be considered in the cost/benefit analysis of fault management are also proposed, including reduction of outage cost, savings in network investments and saving in labor costs.

2.2 State of art on fault location

Currently there are two categories of techniques for estimating the fault location, outage mapping and fault location technique. Outage mapping is a group of techniques that intend to narrow down the area where the fault occurs, based on information from customer calls, circuit breaker status, advanced metering and Geographic Information System (GIS) model [15], [16].

Another category comprises techniques that determine the precise location of fault through calculation using field measurements. Sub-categories of precise location methods are impedance-based methods using sequential network analysis or direct circuit analysis [17]-[22], frequency component-based methods [23]-[25], and methods based on sparse voltage measurements and post-fault power flow analysis [26]-[28].

2.3 Optimized crew management and service restoration

While much work has been done on computer-based fault location [7], a review of literature reveals that the optimization of fault management tasks has not been fully studied yet. The areas that remain inadequately explored include how to interpret the multiple solutions and possible errors from the estimation of fault location, and how to utilize them in the subsequent steps of crew dispatch and necessary post-fault reconfiguration. Current studies on crew dispatch optimization are focused on large-scale or multiple outages, with the purpose of optimizing the process of manually sectionalize the system or restore service after a black-out [29], [30]. Studies on system reconfiguration are based on the assumption that the duration of outage is known, or the

time for reconfiguration is negligible compared to the total time of outage [31], [32]. However these assumptions may not stand in the case of various feeder fault scenarios.

3. PROBLEM FORMULATION

3.1 Introduction to fault management

Faults on distribution feeders are characterized with high frequency and repetitive patterns. Compared to transmission networks, distribution systems have larger size and more complicated operating conditions [8]. Some distribution feeders may be very long in sparsely populated rural areas and frequently must be constructed in adverse environments, especially through wooded areas where tree branches and wildlife may frequently come in contact with the distribution wires, causing both temporary and permanent outages [10]. The degrading of equipment is another contributor to outages especially under severe weather condition.

Fault management aims at minimized the impact of faults to the system and customers. It is consisted with a set of functions—fault detection, fault location, and fault isolation and service restoration [10]. The first two are control-center level functions which are more involved with assistance software, while the other two are field-level functions with switching activities. An overview of FM functions is shown in Figure 1 [11].

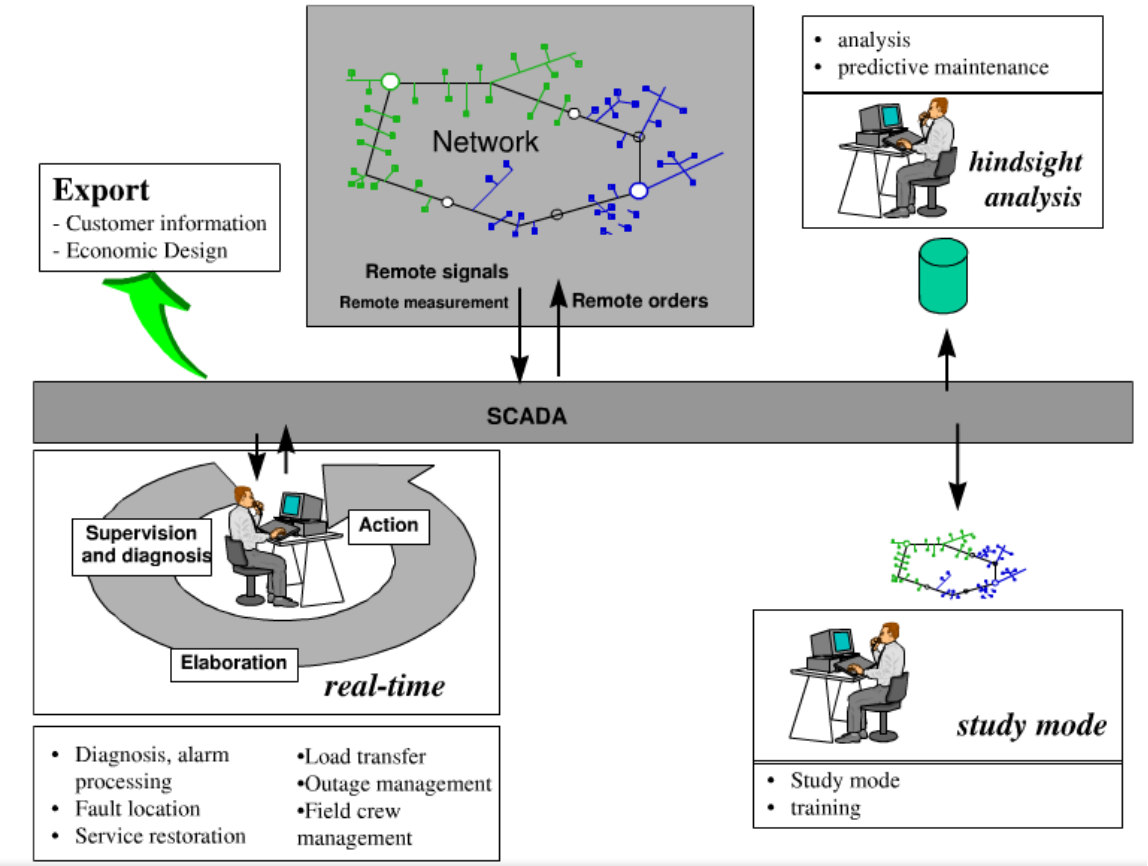

Figure 1 Overview of fault management functions [11]

The essential characteristics of improved fault management are [9]:

- Quicker detection that an outage has occurred
- Accurately determining the location of the fault
- Isolation of the faulted section of a feeder
- Re-energizing the un-faulted sections of the feeder outside the isolation zone, upstream and/or downstream of the faulted section

3.2 Assistance to fault management from new smart grid technologies

A major obstacle for improving the distribution fault management is the lack of monitoring devices installed along the feeders leading to an inability to monitor the system closely in real-time as the faults occur. Consequently, fault management is quite often slow and heuristic. When a fault occurs, it may go unnoticed for some time unless customers report it to the trouble call center. The locating of fault may take long time because repair crew must search along the feeders without a clear instruction where the fault location is and it may be delayed significantly until they visually identify the fault [5].

As a part of Smart Grid deployment projects, Intelligent Electronic Devices (IEDs) are used in monitoring, protection, smart metering systems, and distribution system automation. These smart sensors may be installed in different locations, from substation, along the feeder and down to the customer location. Their data types vary from samples to synchronized phasors, energy measurements and power quality indicators. New fault location algorithms can benefit from this "additional" data and produce more accurate determination of the faulted point [7], which entails the integration and utilization of data collected from various IEDs installed along the feeders [9].

Distribution/Feeder automation is another technology that fastens the process of fault management. As the core of emerging Distribution Automation (DA), remote-controlled reclosers and sectionalizers provide a simple and cost-effective way to automate distribution systems [12]. An example of distribution feeder with DA devices is

illustrated in Figure 2. A circuit breaker is installed at feeder root in a substation. Reclosers R1 and R2 are installed on critical nodes along the main feeder, responsible for isolating permanent faults in the downstream. Sectionalizing switches (or sectionalizers) are installed between reclosers (S2 and S3) and at the beginning of some laterals (S1). These sectionalizers can be operated after the segment of feeder is de-energized by a CB or recloser. They speed up isolation of faulted section and restoration of unfaulted sections through alternate feeder routes. For laterals with light connected load and less significance, fuses at the beginning of the laterals provide protection (Fuse 1 and Fuse 2), and service to downstream loads will not resume until the fuse is replaced after fuse-blows.

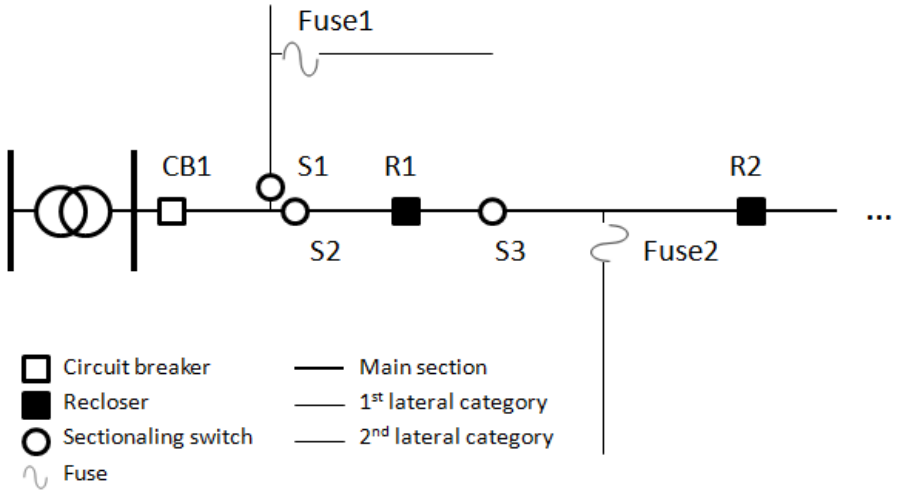

Figure 2 Distribution automation deployment

3.3 Impact of fault management on system reliability

Distribution system reliability is often measured with reliability indices (RIs) [13]. The most important and widely used RIs are System Average Interruption

Frequency Index (SAIFI) and System Average Interruption Duration Index (SAIDI), which represent the average frequency of outages experienced by individual customer, and the average of durations per outage. There are load-oriented RIs such as the Average Service Interruption Duration Index (ASIDI) representing loss to utilities for not being able to send power to the de-energized customers. Besides these RIs for permanent faults, [13] also defines RIs for momentary interruptions, which reflects short-term interruptions caused by transient faults and switching activities. When evaluating the service of utilities, SAIDI and SAIFI are most frequently used.

The impact of FM on system reliability can be assessed by evaluating changes in a comprehensive cost function consists of the related RIs. Formulation of the cost function is based on the cost brought by outages to utilities and customers alike.

3.4 Formulation of the problem

This study provides a solution for improving individual tasks as well as the overall performance of fault management. The benefit is the reduction in the duration and scale of the outage. Reliability indices which are defined to represent different features of outages such as duration, frequency and scale, are used to quantify the cost of outages and assess the benefits.

Flow chart for the proposed fault management is shown in Figure 3. The solid lines indicate sequence of procedures; dashed lines indicate flow of information and knowledge. After a fault is reported, the Outage Management (OM) system first executes fault locating algorithm using field recorded data and system model and identify suspect

locations; the output is then fed to crew dispatch optimization program to create work order and service restoration plan based on the minimum-risk principle. Restoration plan is generated and the benefit of restoration is evaluated to decide whether it is worthwhile or necessary to switch some of the disconnected load to the "healthy" part of the system during the time of repair/replacement.

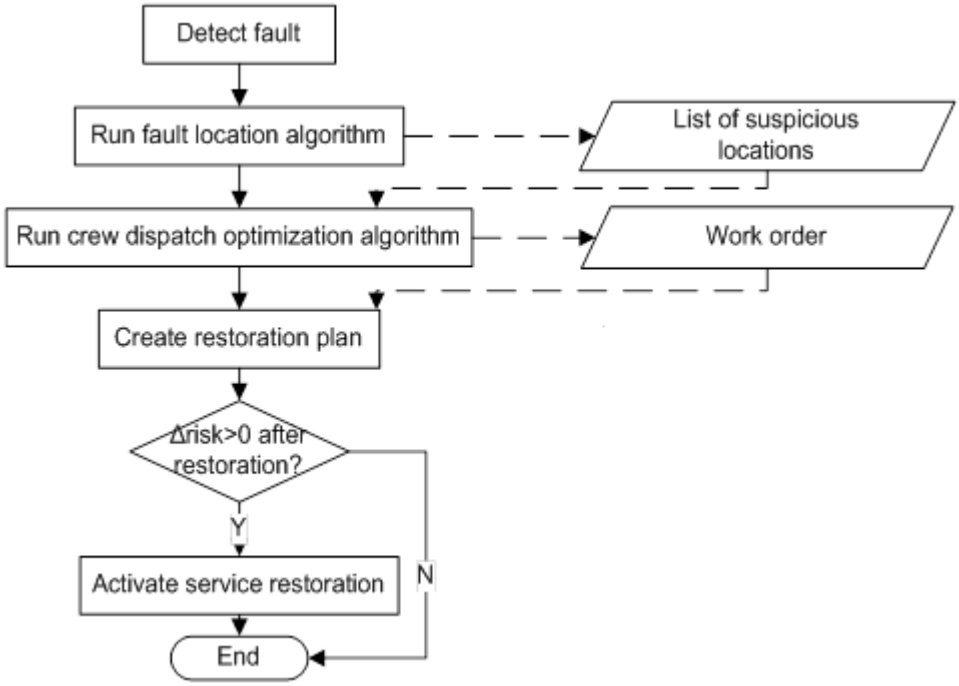

Figure 3 Proposed fault management process

The whole process is based on risk analysis. Deduction of risk from the cost function will be discussed in a separate chapter.

4. RISK-ANALYSIS BASED OPTIMIZATION OF FAULT MANAGEMENT

4.1 Introduction and formulation of outage cost

The cost associated with outages is formulated in many forms. The difficulty lies in quantifying the cost to customers, given the fact that the benefits from reducing the number/duration of outages mostly come to the customers [11]. The commonly used methods to materialize the overall cost include:

- Take full account of customer outage costs as it they were hard costs
- Use certain price per kWh, which is less than the customers' cost but higher than utility's revenue
- Ignore customer cost and focus only on revenue

In this research, the second method is used to include customer outage cost into the cost function.

Customer based reliability index SAIDI (System Average Interruption Duration Index) and load based reliability index ASIDI (Average System Interruption Duration Index) defined in [13] are used to quantify the improvement. Definitions of these indices are:

$$SAIDI = \frac{\sum r_i N_i}{N_T} \tag{4.1}$$

$$ASIDI = \frac{\sum r_i L_i}{L_T} \tag{4.2}$$

where

i is the index number of an interruption event;

r_i is duration of interruption i;

N_i is number of customers interrupted by interruption i;

L_i is connected load in kVA interrupted by interruption i;

N_T is total number of customers;

L_T is total connected load in kVA.

Moreover, according to the emerging power quality regulation [14], utilities that fail to pass the minimum threshold of power quality (usually defined in terms of yearly SAIDI value) will have to pay penalty to ISOs, as a drive to improve their service.

Taking into the account of penalty, the overall cost of outage is given as:

$$\begin{aligned} \text{C}ost &= PR \cdot g(SAIDI, SAIDI_{Tgt}) + ER \cdot ASIDI \cdot L_T \\ &= PR \cdot g(SAIDI, SAIDI_{Tgt}) + \sum_i ER_i \cdot T_i \cdot L_i \end{aligned} \tag{4.3}$$

whereSAIDI and ASIDI are the reliability indices defined in;

i is the index of one interruption event;

T_i is the duration on one interruption event;

L_i is the affected load in kWh;

L_T is the total connected load in kWh;

$SAIDI_{Tgt}$ is the target value of yearly *SAIDI;*

PR is penalty rate for SAIDI to exceed $SAIDI_{Tgt}$;

ER is the price associated with loss of load per kWh;

and g(x,y) is a function defined as:

$$g(x,y)=\begin{cases} x-y, & x>y \\ 0, & x\le y \end{cases} \tag{4.4}$$

It is worth noticing that the price *ER* varies with different customers, according to their willingness to pay for better service [11]. Typically *ER* is higher with industrial and commercial customers, and lower with residential and agricultural customers.

4.2 Formulation of risk function

On the stage of fault management, the yearly SAIDI is very hard to predict because of the randomness and low rate of outages in a year. The risk associated with a fault management function is defined as follows, with the penalty part assumed as 0:

$$\begin{aligned} Risk &= E[\text{Cost}] = \sum_i P_i \cdot Cost_i \\ &= \sum_i P_i \cdot (ER_i \cdot T_i \cdot L_i), \quad and \ \sum_i P_i = 1 \end{aligned} \tag{4.5}$$

where P_i is probability of consequence i from the fault management task, and $\Sigma P_i=1$ means that all possible consequences are considered. $Cost_i$ is the total disconnected load L_i times duration T_i, or the loss in kWh associated with consequence i.

The cost function $Cost_i$ represents the deterioration of system reliability by consequence i. From utility point of view, *Costi* is directly related to the revenue loss; from customer point of view, $Cost_i$ reflects the length of experienced outage; from system point of view, $Cost_i$ reflects the severity of outage, both in length and range.

The importance of the affected customers is also a factor, although it is not shown in the equation. For example, failing to supply power to a hospital or an industrial customer has a more severe consequence than failing to supply a residential area, and

penalties are often paid by utilities to such customers according to their contracts for not meeting the pre-agreed requirements. The importance of customers can be factored in by assigning different value of ER to different loads in (4.5).

4.3 Fault management functions of interest

Two functions can be optimized given the improved fault location in Section 4: crew dispatch and service restoration.

With the unique output from the proposed fault location method, system operator can prioritize the nodes for field inspection conducted by crews. In general, lateral sections with higher probability to contain the true location of fault should be inspected first, and vice versa. Optimized crew dispatch aims at combining the fault location output with the risk function to find the best dispatch plan.

Service restoration aims at finding the best switching scheme with no knowledge of how long an outage will last, by studying the pattern in outage cost in relation with pattern in faults, time associated with control and operation activities, and different candidate switching schemes.

4.4 Conclusion

In this section, the outage cost function is defined and used to formulate the risk used in the optimization problem, after analysis of the impact of outage to customers and utilities, and the commonly used method for assessing the outage cost. Penalty from the power quality regulation is added in the outage cost to factor in the urge of improving

system reliability on a supervision and regulation level. Fault management functions that can benefit from the improved fault location and optimized through the risk function have been addressed. Detail of the optimization is given in the following sections.

5. IMPROVED FAULT LOCATION METHOD*

5.1 Introduction

The urge for a better fault location method is from the fact that the smaller the area for crews to inspect in the field, the less time it takes to actually locate the fault. However better fault location methods require more supporting information from the system, and more than often that means more sensors to be installed and new communication paths to be established. Through risk-based analysis the improvement in system reliability in terms of dollars can be compared with the investment spent on sensors and communication paths, so that utilities have a measure to decide whether the implementation of a new method is beneficial. In this section a new fault location method is proposed, as an example as to what extent the accuracy can be improved through utilization of new data.

5.2 Voltage measurement-based methods

The voltage measurement-based method is first proposed by Galijasevic and Abur in [26], where the concept of vulnerability contours is used in assessing the likelihood of voltage sags effecting a given network area. In [27] Pereira, et al. extended the formulation in [26] assuming the availability of voltage and current phasors at feeder root, and voltage sag measurements from sensors along the feeder. Voltage sags were calculated using a post-fault load flow approach that doesn't require the estimation of

---

fault resistance. In [28] Lotfifard et al. assumed post-fault phase angle shifts being available from sparse measurements, and proposed an approach for eliminating some tentative nodes by characterizing the voltage sags from different sensors. New index was proposed for analyzing voltage sags and angle shifts calculated from the load flow computation based on estimated fault resistance.

5.3 Pereira's Algorithm [27]

The fault location method from [27] is based on the fact that different drops in voltage amplitudes (voltage sags) are experienced by each feeder node during a fault. The algorithm runs the pre-fault load flow first, then assigns one node as the faulted node, runs post-fault load flow, calculates voltage sags, and calculates difference (mismatch) between calculated and measured values. When faults on all tentative nodes have been simulated, the tentative node with smallest mismatch is selected as output.

The core of Pereira's algorithm is the calculation of load flows. An iterative load flow algorithm for radial distribution system described in [33] is used to solve pre-fault load flow. Back-sweeping to update branch currents using (5.1) and (5.2) and forward-sweeping to update node voltages using (5.3) are conducted in each iteration. The stopping criterion for iterations is defined by (5.4).

$$I_{j\_n}^{(k)} = Z_{L\_n}^{-1} \cdot V_n^{(k-1)} \tag{5.1}$$

$$I_{b\_i}^{(k)} = \sum I_{b\_p}^{(k)} + I_{j\_n}^{(k)} \tag{5.2}$$

$$V_n^{(k)} = V_m^{(k)} - Z_{b\_i} \cdot I_{b\_i}^{(k)} \tag{5.3}$$

$$\max\left\{\left|V_n^{(k)} - V_n^{(k-1)}\right|\right\} < \varepsilon \quad , \text{ n=1,…,N} \tag{5.4}$$

where k is the number of iteration, $I_{j\_n}^{(k)}$ is the injection current at node n, Z_{L_n} is the three phase load impedance matrix at node n, $V_n^{(k)}$ is the node voltage of the down-stream node of branch i, $I_{b\_i}^{k}$ is the branch current of branch i, which flows from node m to node n, $I_{b\_p}^{(k)}$ is the branch current of branch p, which flows out from node n, Z_{b_i} is the three phase line impedance matrix for branch i, ε is the threshold for change in node voltage, and N is the total number of nodes.

In post-fault load flow computation similar procedures are used, except that the mismatch between measured and calculated values of feeder current is calculated after calculation of branch currents (5.5), injected to the assumed faulted node (5.6), and the branch current is updated again using (5.2).

$$I_f^{(k)} = I_m^{df,meas} - I_m^{df,cal(k)} \tag{5.5}$$

$$I_{j\_n}^{df,(k)} = I_{j\_n,L}^{df,(k)} + I_f^{(k)} \tag{5.6}$$

where $I_f^{(k)}$ is fault current, $I_{rn}^{df,meas}$ is the during-fault current measured at feeder root, $I_{rn}^{df,cal(k)}$ is the calculated current at feeder root, $I_{j\_n}^{df,(k)}$ is the injection current at faulted node n, $I_{j\_n,L}^{df(k)}$ is the injection current from load connected to n.

5.4 Limitations in Pereira's Algorithm

Pereira's approach smartly bypassed the estimation of fault resistance. However it introduced confusion when no measurements are taken from the downstream of the faulted node. This can be explained by circuit analysis. Figure 4 below depicts such a case. V_r and I_r are voltage and current phasors at feeder root. The dotted box represents the unfaulted part of the feeder, which contains all the measurement nodes (M_1 to M_m). Zb1 is the branch impedance between node i and i+1, Z_{L1} and Z_{L2} are load impedance connected to node i and i+1. $Z_{L\Sigma}$ is the equivalent impedance of branches and loads behind node i+1.

The network between node 1 and node i can be represented as a two-port network:

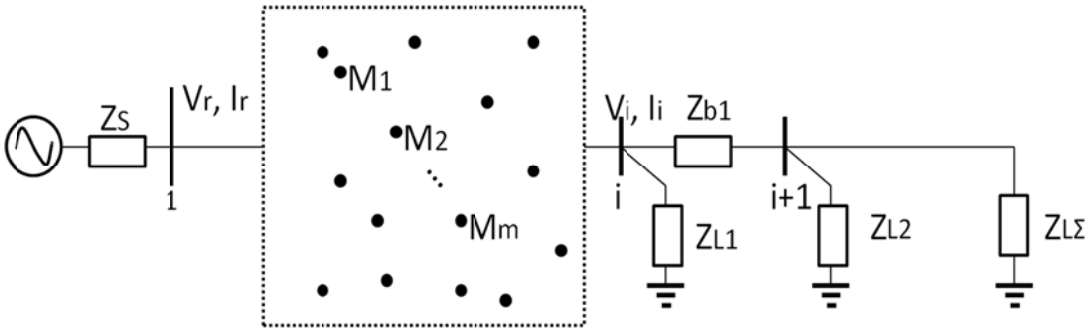

Figure 4 One-line diagram of a feeder

$$\begin{bmatrix} V_r \\ V_i \end{bmatrix} = \begin{bmatrix} Z_{rr} & Z_{ri} \\ Z_{ir} & Z_{ii} \end{bmatrix} \begin{bmatrix} I_r \\ I_i \end{bmatrix} \tag{5.7}$$

Without loss of generality, a fault is assumed at node i with fault resistance of R_f. V_i can be represented by I_i and R_f:

$$\begin{cases} V_i = Z_{equ} \cdot I_i \\ Z_{equ} = R_f \parallel Z_{L1} \parallel [Z_{b1} + (Z_{L2} \parallel Z_{L\Sigma})] \end{cases} \tag{5.8}$$

Now consider the situation that the fault location software put "fault" at node i+1. The process of during-fault load flow equals to that of putting an impedance of Z_x at node i+1 and tuning it to get the same Z_{equ}:

$$Z_{equ} = Z_{L1} \parallel [Z_{b1} + (Z_{L2} \parallel Z_{L\Sigma} \parallel Z_x) \tag{5.9}$$

which yields to:

$$Z_x = -\frac{Z_{b1} - Z_{equ1}}{Z_{b1} + Z_{L2}Z_{L\Sigma} - Z_{equ1}} \cdot Z_{L2}Z_{L\Sigma} \tag{5.10}$$

$$Z_{equ1} = \frac{R_f + Z_{b1} + \dfrac{Z_{L2}Z_{L\Sigma}}{Z_{L2}Z_{L\Sigma}}}{R_f \cdot (Z_{b1} + \dfrac{Z_{L2}Z_{L\Sigma}}{Z_{L2}Z_{L\Sigma}})} \tag{5.11}$$

When $R_f=0$, we have $Z_x = -\dfrac{Z_{b1}Z_{L2}Z_{L\Sigma}}{Z_{b1} + Z_{L2}Z_{L\Sigma}}$. Assuming load impedances to be high enough to be neglected and apply $Z_{b1}/(Z_{L2}Z_{L\Sigma}) \approx 0$ we have $Z_x \approx -Z_{b1}$.

Figure 5 shows the angle and amplitude of Z_x with different R_f and $|Z_{b1}|$ when $\angle Z_{b1}=60°$. It can be seen that although $\angle Z_x$ changes significantly with different settings of R_f and $|Z_{b1}|$, the angle is always negative (impedance vector in 3rd and 4th quadrant).

Similar analysis has been done to cases where Z_x is connected to nodes before node i, and the conclusion is that the angle of Z_x is closest to 0° when it is connected to the actual location of fault.

The above discussion reveals that Pereira's algorithm is not capable of differentiating neighboring or serial nodes in some cases because representation of Z_x is not considered.

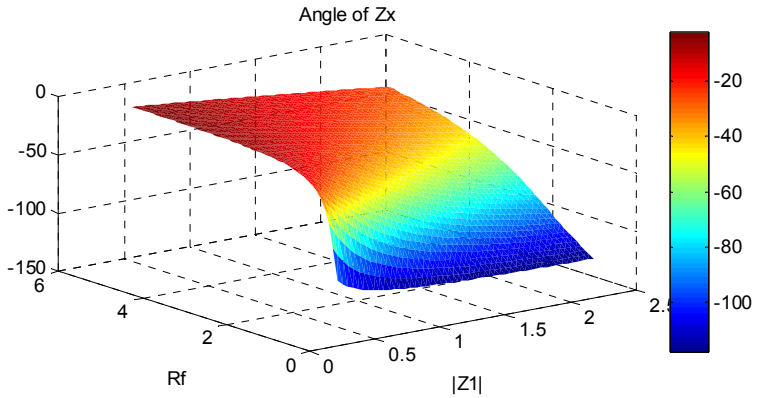

Figure 5 Z_x with different R_f and $|Z_{b1}|$, $\angle Z_{b1}=60°$, $Z_{L2}\rightarrow inf.$, $Z_{L\Sigma}=500\angle 30°$

5.5 Proposed fault location method

5.5.1 Description of procedures

The proposed fault location approach utilizes voltage and current phasors from the root of a feeder and the magnitude of voltage sags from sparse sensors with voltage measurements such as Power Quality Meters. Synchronization or phasor angle information is not required. The feeder is divided into several segments based on the placement of protective devices.

The proposed fault location scheme is illustrated in Figure 6. The upper left of the figure is a diagram of a distribution feeder with segmentation and location of

measurements. At the beginning of fault location process, DT-based segment identifier receives the measurements and identifies the faulted segment. The segment information is then passed on to the function block of faulted node selector, where fault is simulated at every node in the identified segment, and the scenario producing the smallest difference between simulated and measured quantities is selected as the output.

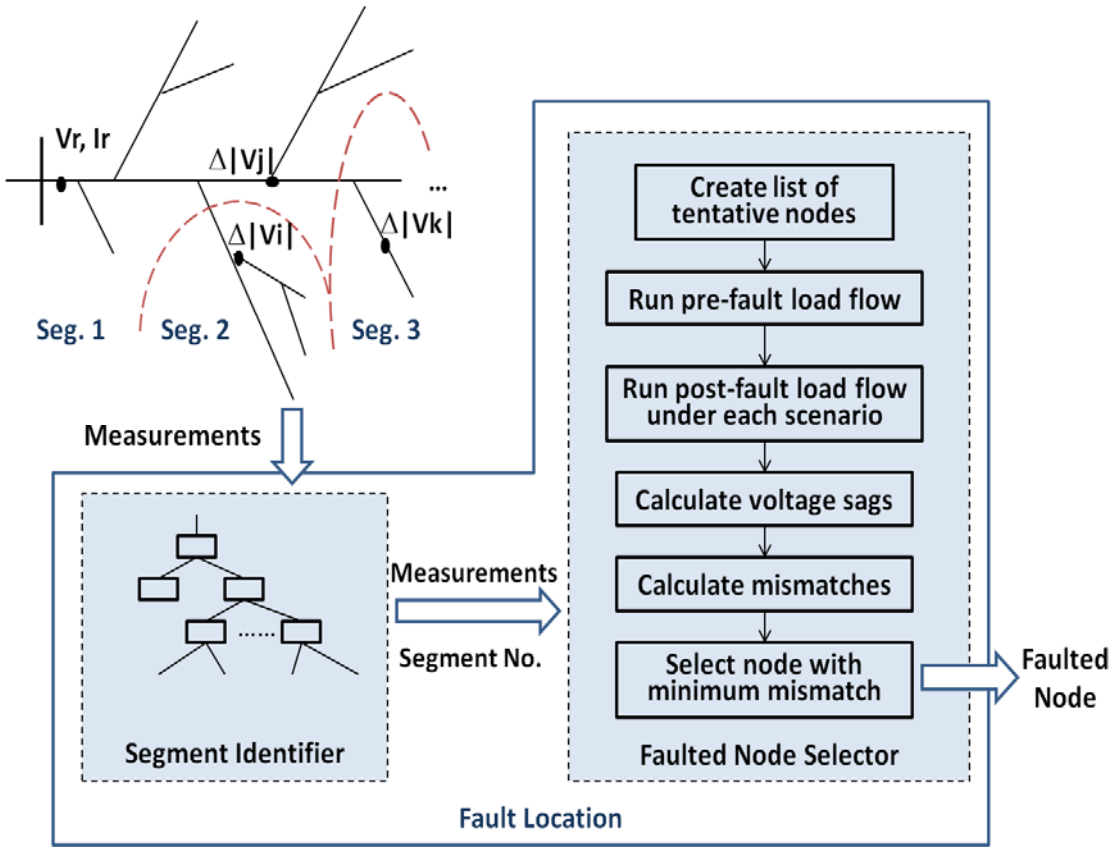

Figure 6 Procedures of the proposed fault location scheme

5.5.2 Decision-Tree based segment identifier

In classification analysis, a case consists of instance (x, y) where x is the vector of attributes and y is the target. The relationship between x and y is usually described by a classification function, through which it is possible to estimate how the target y

changes when x is varied. In our proposed approach, the classification function is realized by a binary tree structure, where x is the vector of measurements used for fault location and y is the fault segment ID.

In this work the commercial data mining software CART [34] is used to develop the classification trees. The approach in CART to build a DT entails three steps:

1) tree growing using a learning dataset;
2) tree pruning using cross-validation or an independent validation dataset;
3) selection of the best pruned tree. The DT growing, node splitting, tree pruning and optimal tree selection algorithms are detailed in [35], [36]

Experimental tests show that there is a trade-off between tree complexity and its accuracy: a small-sized tree may not be able to capture enough system behavior, and a large-sized tree may lead to imprecise prediction due to its over-fitting model. In this work the rule of minimum cost regardless of size to search for the best pruned DT commensurate with accuracy is adopted. The complexity cost parameter in CART has been set to zero.

5.5.3 Faulted node selector

Based on the conclusion from Section 5.4 a new criterion for selecting the faulted node is proposed:

$$error_j = \frac{\sum_{i=1}^{m} \left| \Delta V_{M,i}^{meas,j} - \Delta V_{M.i}^{calc,j} \right|}{V_N} + \alpha \frac{\left| \angle Z_x^j \right|}{2\pi} \qquad (5.12)$$

where $error_j$ is the mismatch associated with node j assumed as faulted node, $\Delta V_{M,i}^{meas,j}$ is the measured voltage-sag amplitude at the ith measurement node, $\Delta V_{M,i}^{calc,j}$ is the calculated voltage-sag amplitude at the ith measurement node, V_N is the rated voltage, α is the weight factor for angle index, $\angle Z_x^j$ is the angle index in radius, calculated from

$$\angle Z_x^j = \angle V_j^{calc,j} - \angle I_f^{calc,j} \tag{5.13}$$

where $\angle V_j^{calc,j}$ and $\angle I_f^{calc,j}$ are the calculated angle of node voltage and fault current at node j.

Node with the smallest value of $error_j$ will be selected as the algorithm output. The optimal value of α from Eq. (5.12) is highly dependent on the accuracy of input measurements and the system model. Typically, if the model parameters are close to actual values from the field and the number of voltage measurements is small, or the voltage measurements contain high level of error, a larger weight factor should be assigned to the angle index. When the measurements are accurate but a simplified model is used, smaller value of weight factor will produce better result.

5.6 Conclusion

This section addressed the constraint of a state-of-art fault location method through a theoretical analysis. A two-step fault location method is proposed to improve the accuracy while reducing the computational burden. Decision tree is applied in identifying the segmentation where a fault occurs, and new index for selecting the faulted node is proposed to avoid confusion that exists in the previous method.

6. OPTIMIZED CREW DISPATCH

6.1 Introduction

The necessity of optimizing crew dispatch comes from the ambiguity/mismatch of results from fault location software. This may happen for various reasons:

- Fault location algorithm error. One example is that R1 in Figure 2 is opened to isolate the fault but the software locates
- The fault as being behind Fuse 2 due to an error in the input or system model
- Coordination problem between protection equipment. For example, when a fault occurs behind Fuse 2, R1 operates before Fuse 2 burns out
- Mal-function of protection equipment. For example, fault is actually behind R2 but R2 failed to open, so R1 clears the fault after a time delay

In the meantime, the proposed fault location method is capable of providing a list of nodes with descending probability of being the true location of fault. It is observed that the true node is not always the first one on the list, due to the error in measurements, load estimation and model parameters, but it's always on the top, with its neighboring nodes before and after it. It is possible to form several (for example, 2) geometrical areas as candidates, and optimize the number of crews and sequence of inspection based on the risk function [37].

In the formulation of the optimization problem of crew dispatch, scenarios of multi-faults are not considered due to their rareness.

6.2 Formulation of the crew dispatch optimization

Formulation of the crew dispatch optimization is as follows:

$$Min.\left\{Risk(node\,1,...node\,M;\, N_{labor.1},...N_{labor.j})\right\}$$

$$s.t.\quad \sum_{j=1}^{i} N_{labor.j} = N_{labor.\max} \tag{6.1}$$

where node 1 to node M are nodes in Area 1 through Area i, i is the number of areas that needs inspection, divided by protective devices, $N_{labor.j}$ is the number of dispatched crews to area j, and $N_{labor.max}$ is the total number of available crews.

Since the disconnected part stays the same when crews are searching for fault, the optimization problem in (6.1) can be rewritten as

$$Min.\left\{\sum_{i} P_i \cdot T_i \,|\, node\,1,...node\,M;\, N_{labor.1},...N_{labor.j}\right\}$$

$$s.t.\quad \sum_{j=1}^{i} N_{labor.j} = N_{labor.\max} \tag{6.2}$$

6.3 Calculation of P_i and T_i

In (6.2) P_i is now the probability that fault is in Area i, which comes from the ranking of nodes in Area i from fault location computation.

T_i is the estimated time for locating the fault given the arrangement of crews. Figure 7 shows the composition of T_i when i=2. Figure 7(a) and (b) are two possible consequences for one serial inspection plan: send all crews to area 1, and if fault is not in area 1, continue search in area 2. This is a candidate plan when the probability that fault

is in area 1 is larger than that it is in area 2. T_0 is the travel time, which is proportional to the distance between maintenance office and inspection area. T_1 is estimated time to find fault if it is in area 1, which is determined by the size of area 1. T_1' is time to search the entire area 1, and T_2 is estimated time to find fault if it is in area 2. Another option is a parallel inspection, in which crews are split to groups and inspect the two areas in parallel, as is in Figure 7 (c). In this case estimated time to find the fault in the two area is T_1" and T_2" separately, and the total time is composed of T_0 and the smaller number of T_1" and T_2".

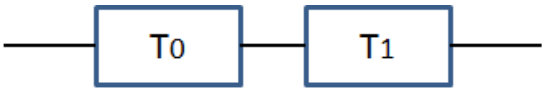

(a) Serial inspection with fault in area 1

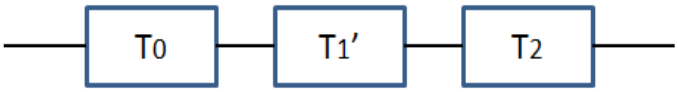

(b) Serial inspection with fault in area 2

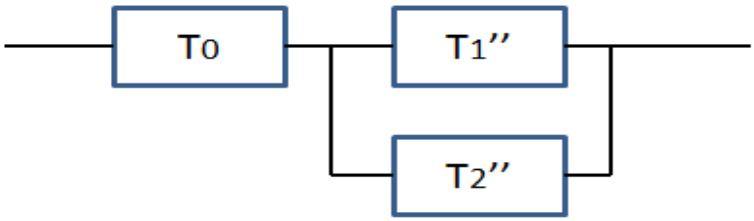

(c) Parallel inspection

Figure 7 Composition of T_i

6.4 Conclusion

Formulation of the optimization in crew dispatch is given in this section, together with approach for calculating the factors in the equation. Implementation of crew dispatch will be discussed in the section of case study.

7. OPTIMIZED SERVICE RESTORATION

7.1 Introduction

With the distribution automation deployment, remote-controlled or automated switching is capable of isolating the faulted section with the rest of the feeder, and resume service to the downstream customers via alternative routes before the faulted component is repaired or even before the fault has been visually confirmed by field crews. The centralized FM is capable of coordinating complicated switching activities, including opening of sectionalizing switches, closing the fault-tripped CBs or reclosers, and closing the normally-open CBs installed at the end of the laterals to get power from neighboring feeders.

With different level of distribution automation, speed for performing different steps of service restoration is different in different FM deployments. Excessive cost may be introduced to the outage cost by the switching activities. One major problem is that customers on the healthy feeder which provides backup power supply to the disconnected customers will lose power during the switching process, both when the alternative route is established by closing the CB, and when it's revoked and system resumes to normal state. Typically the longer an outage lasts, the more beneficial a service restoration is.

A reconfiguration optimization problem can be formulated as follows:

$$\begin{aligned} &Min.\ \{\Delta L, N_{SW}\} \\ &s.t. \quad V_{\phi\min} \le |V_{\phi}| \le V_{\phi\max} \\ &Max.\{|P_A - P_B|, |P_B - P_C|, |P_C - P_A|\} \le \Delta P_{\max\_imbalance} \end{aligned} \tag{7.1}$$

$$P_{Ti} \le P_{Ti\_\max}$$
$$\left|P_{i-j}\right| \le \Delta P_{\max\_i-j}$$

where

ΔL: total disconnected load after reconfiguration;

N_{SW}: number of switching operations;

V_{Φ}, $V_{\Phi min}$, $V_{\Phi max}$: phase voltage and its lower and upper limits;

P_A, P_B, P_C: total load connected to phase A, B and C;

$\Delta P_{max\_imbalance}$: upper limit of load imbalance;

$P_{Ti}, P_{Ti\_\max}$: load connected to transformers and the transformer capacity;

$\left|P_{i-j}\right|, P_{\max\_i-j}$: power flow (non-directional) on branch i-j and the line capacity.

Once system operator decides to do service restoration, optimal plan is found by solving the optimization problem of (7.1).

Currently service restoration is either performed automatically after every outage with no exception, or based on the operator's estimation on how severe the situation is and their own experience. An example of such a decision-making strategy is "if loss of load is more than 1000kW then generate the reconfiguration plan and do system reconfiguration".

There is cost associated with reconfiguration too. The cost comes from following aspects:

- Customers connected to the unfaulted part may be affected by switching activities;
- Switching adds time to the duration of outage, and the time is doubled when original topology is resumed later on;
- Reconfiguration is constrained by the connectivity of the system and load capacity of the unfaulted part;
- Switching operations reduce the service life of protective devices, especially CBs and reclosers.

Thus another problem should be solved besides how to reconfigure the system: what is the optimal strategy of reconfiguration.

7.2 Formulation of optimization problem

The optimal service restoration sloution is the one which can most effectively reduce Risk. When the duration of an outage is known, the reduction in risk can be calculated:

$$\begin{aligned}\Delta Risk &= (T_1 \cdot L_1) - [T_{COM} \cdot L_1 + 2I_{SWC} \cdot (L_1 + L_2 + L_3) + \\ &\quad + (T_1 - T_{COM} - T_{SWC}) \cdot (L_1 - L_{REC})] \\ &= (T_1 - T_{COM} - T_{SWC}) \cdot L_{REC} - T_{SWC} \cdot (L_1 + 2L_2 + 2L_3)\end{aligned} \tag{7.2}$$

where

T_1 is the time of outage;

L_1 is the total load that lost power due to a fault;

T_{COM} is the time needed for computing reconfiguration schedule for (7.2);

T_{SWC} is the time needed for switching;

L_{REC} is the total loads that regain power by reconfiguration;

L_2 is the loads connected to the section between the opened sectionalizer and the immediate upstream recloser;

L_3 is the load in the unfaulted part where L_{REC} is connected to.

With this formulation, $\Delta Risk>0$ means the reconfiguration is beneficial.

For an outage caused by a fault, most of the time T_1 is unknown before the crews find out the actual location of the fault and the cause in the field. There is no effective way of estimating outage time without determining the cause of outage [2]. Therefore solving (7.2) analytically becomes very difficult. Instead a predictive method using Monte Carlo simulation for finding $\Delta Risk$ is proposed, as is shown in Figure 8. First a set of reconfiguration strategies are prepared. Monte Carlo simulation generates random faults based on the probability model of faults. Information such as loss of load (L_1) and status of protective devices is feed to the reconfiguration strategies, which produces T_{SWC}, L_{REC}, L_2 and L_3. T_{COM} is considered constant. Together with T_1 from Monte Carlo simulation, $\Delta Risk$ can be calculated using (7.2). If decision from a strategy is "no reconfiguration", then $\Delta Risk$=0. After several rounds of simulation the means of $\Delta Risk$ associated with different strategies converge, providing criteria for comparison between strategies.

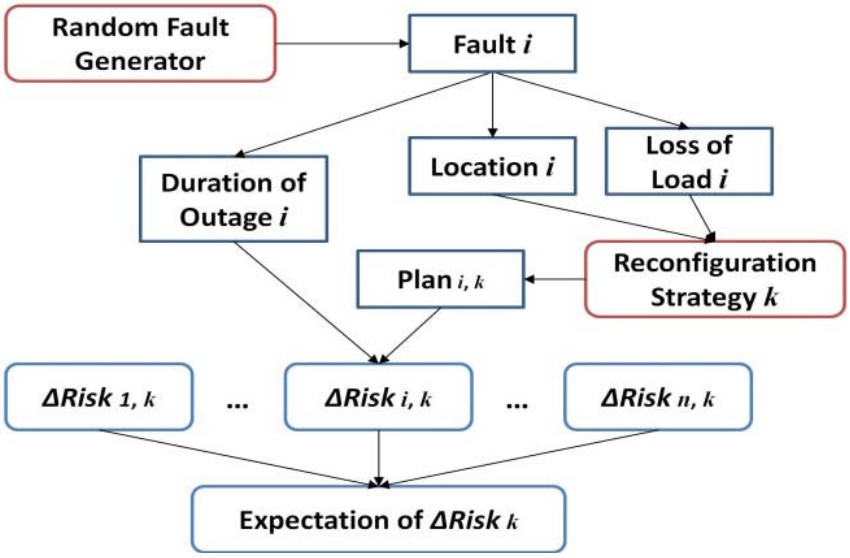

Figure 8 Procedures for estimating *ΔRisk*

Approach for generating the stochastic fault model is given in the section of case study.

7.3 Conclusion

Formulation of the optimization in service restoration is given in this section. Transform of the original risk function is deduced. Due to the lack of knowledge on the duration of outage, an analysis based on stochastic process is proposed.

8. APPROACH TO THE ASSESSMENT OF BENEFITS

8.1 Introduction

The benefit obtained from the improved fault management functions is assessed through the improvement in yearly outage cost, which is defined in equation (5.3). The improvement is defined as profit:

$$\text{Profit} = PR \cdot \Delta g(SAIDI, SAIDI_{Tgt}) + ER \cdot \Delta ASIDI \cdot L_T \qquad (8.1)$$

The difficulty of calculation the profit lies in calculation of the RIs.

8.2 Calculation of profit

Reliability indices are calculated using stochastic method. Due to the differences between fault scenarios (duration, affected phases and loads, error from fault location method, switching capacity, etc.), it is difficult to build one probability model for fault management activities, which makes direct calculation of reliability indices impossible. Therefore stochastic process is introduced.

Monte Carlo simulation is used in this study to generate fault scenarios that follow the probability model of faults and then let fault management deal with each scenario. Reliability indices are calculated at the end of each simulation cycle (one year period) until their means converge. The means are used in calculation in (8.1). Another merit of this approach is that variances of the indices are also calculated, allowing operators to evaluate the impact of fault management activities on the stability of reliability indices.

A detailed description of the Monte Carlo simulation is recorded in Section 9. Following assumptions has been made in the setup.

- Failure rates in two weather states are used to simulate faults in normal weather days and adverse weather days;
- Under each weather condition Time To Next Fault (TTNT) follows a Homogeneous Poisson Process (HPP);
- Location of fault follows a uniform distribution;
- Hours are counted separately for good weather days and bad weather days to determine the occurrence of a fault;
- Causes of faults are different in the two weather types and lead to different repair time (RT) (Figure 9);
- Outage time is built by combining the travel time, inspection time and repair time (Figure 10). In case of system reconfiguration, sum of the three forms T1.

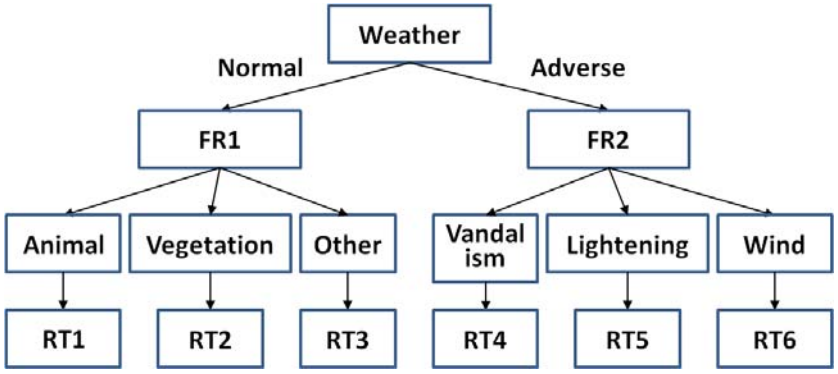

Figure 9 Generation of fault scenarios

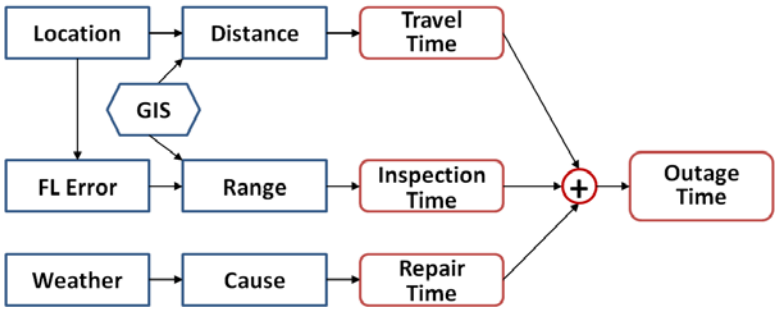

Figure 10 Calculation of the outage time

8.3 Conclusion

In this section, profit defined by the reduction in outage cost is used as the index for assessment of benefits. Approach for calculation of the profit is proposed through utilization of Monte Carlo simulation. The stochastic method is also used in the optimization of service restoration strategy.

9. IMPLEMENTATION OF THE PROPOSED STUDY

9.1 System model

The proposed fault location method and fault management optimization approach has been implemented on a 13.8 kV, 134-node, overhead three-phase primary distribution feeder shown in Figure 11 [37], [39]. Total length of the main section of the feeder is 432 km. Total length of first and second category laterals is 267 km and 261km respectively. The average length of a branch (line between two neighboring nodes) is 7.2km. Details of the test system can be found in Appendix.

Non-transposed line model with lumped parameters were used, and loads were modeled as constant impedances in the ATP simulations [39]. Root voltage and current are measured at node 1. Six voltage measurements are placed along the feeder, at node 23, 30, 63, 79, 96 and 112 respectively (marked as M in Figure 11). The feeder is divided into 12 segments based on the placement of reclosers and sectionalizing switches (numbered with dotted curves in Figure 11).

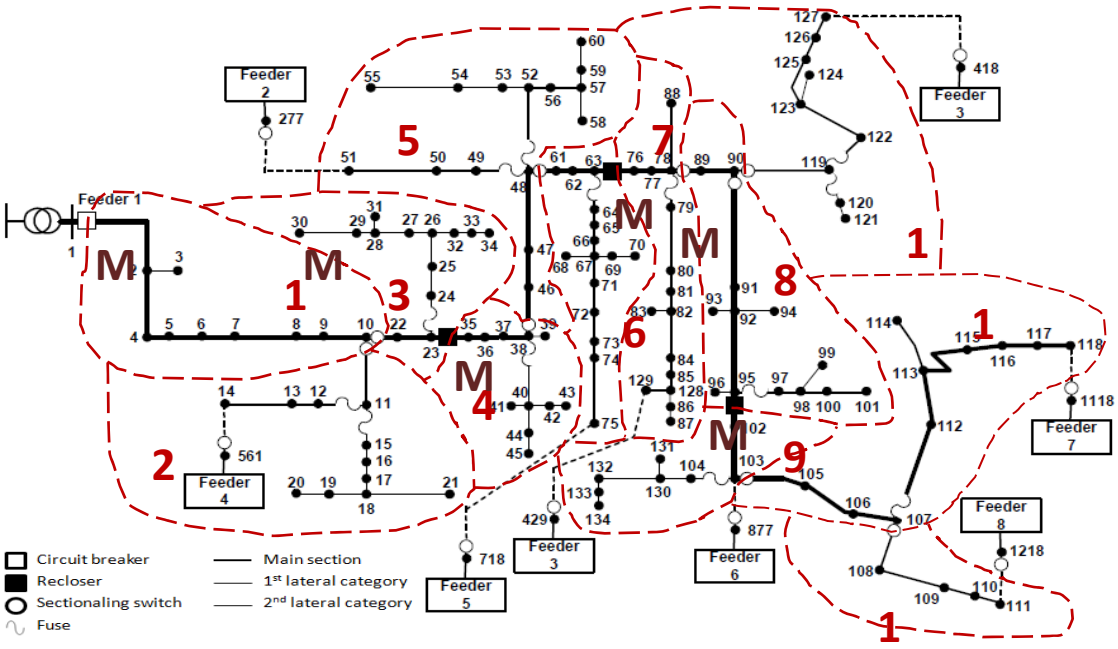

Figure 11 Topology of the 13.8 kV, 134-node, overhead distribution system

9.2 Implementation of fault location method

9.2.1 Generation of knowledge base

The knowledge base is a database used for off-line training of the DT-based segment identifier. It is composed of a number of instances, and each instance represents a fault scenario and is labeled with corresponding fault segment ID. Typically, the DT-based identification model will gain more generalization power if a larger number of instances are included in the knowledge base [40], [41]. However the database generation process should be properly designed, otherwise it will not capture sufficient information from the entire problem space.

In this work the distribution system shown in Figure 11 is modeled in ATP. In order to create a sufficiently large knowledge base, add-on scripts for scenario generation

have been developed using hybrid programming between MATLAB and ATP. The function takes the original ATP model as a reference model, automatically inserts fault scenario settings into switch and impedance data cards (faulted node, and fault resistance), saves modified model in a separate ATP file and calls execution file "tpbig.exe" to run simulation in ATP. When ATP simulation is complete, the output file from ATP (.pl4 file) is converted to MATLAB data file (.mat file) by calling "pl42mat.exe", the phasors from feeder root and voltage sags at measurement nodes are calculated in MATLAB and stored with fault information. The process of generating one fault scenario is shown in Figure 12. The arrows in the left hand side block illustrates the sequence of MATLAB functions, arrows in the right hand side block shows the information flow between outside files, and the dashed arrows in between shows the calling and returning of outside files.

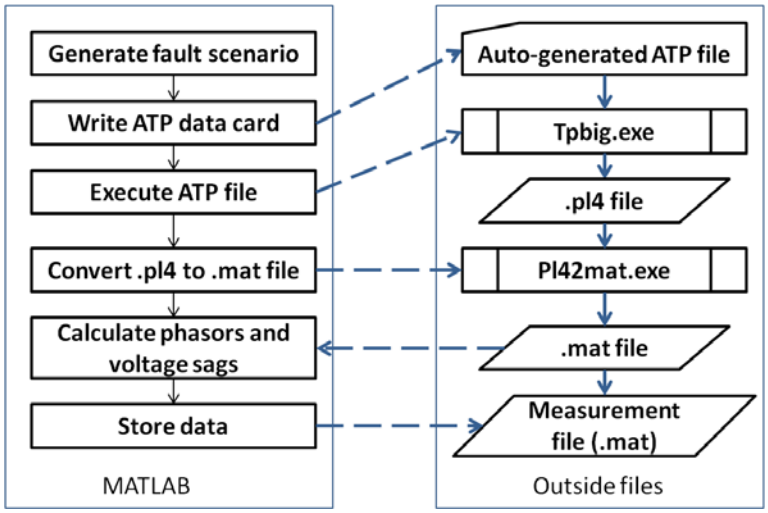

Figure 12 Procedure of knowledge base generation

9.2.2 Training of the decision tree

A knowledge base comprising 49210 fault scenarios is used for DT training. Random errors following a normal distribution with zero mean and deviation of 0.5% are added to the measurements of each scenario to mimic situation in real world. Settings of fault scenarios include fault resistance, faulted node and pre-fault load pattern. Faults along the feeder (node 2 to 134), with fault resistance of 0 to 30Ω are simulated. Loads are classified into residential and business, and load variation is achieved by varying the load impedance based on an hourly load forecast of the different types of load.

The 10-fold cross-validation method is used to develop the classification tree in CART. The topology of resulting optimal tree is shown in the middle of Figure 13. The block above the tree shows details of the four nodes at the top layers. Details of one terminal node are shown in the block on bottom-right. The label of a terminal node is determined by the majority of training cases falling into that node. In this example 50 of the training cases reached the terminal node and they all belong to Class 2. In online applications, the measurements of a fault will be fed into the tree and go through a particular top-down path. Once they reach one terminal node, the faulted segment can be immediately identified.

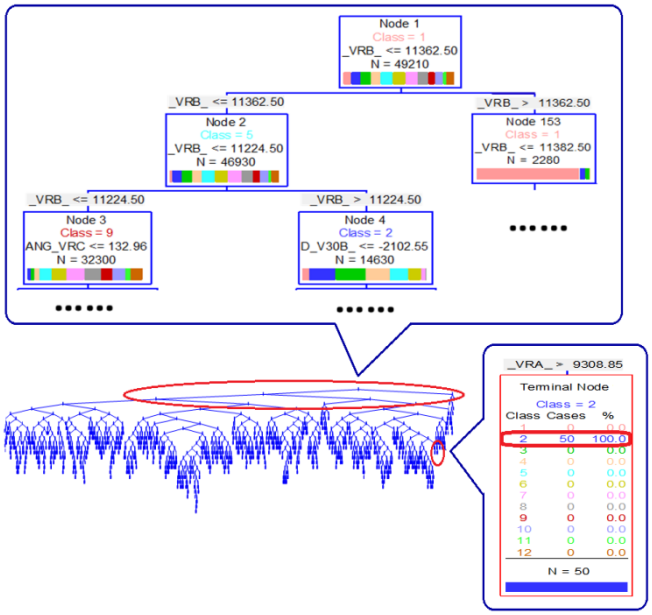

Figure 13 Decision Tree topology for segment identification

9.2.3 Implementation of faulted node selector

Programming for locating fault is done in MATLAB. The optimal weight factor of α is determined by the following procedures: 1) vary α in the range of 0 to 0.1; 2) feed the fault location program with no-error measurements and record the output error; 3) fit the sets of α and output errors to a polynomial curve; 4) find the extreme point on the curve and record α. The optimal α is determined as 0.031. Both the algorithm reported in [27] and the proposed algorithm are implemented and the results have been compared in Section 10.

9.3 Implementation of Monte Carlo Simulation

A similar process as was described in [42] has been implemented, with reliability-related settings described in Table 1.

Table 1 Settings for Test Scenarios

Average normal weather hours: 724; Average adverse weather hours:4
Two-state Failure Rate (/year): FR1=1, FR2=50
Probability Model for Hours of Normal Weather: Gaussion
Probability Model for TTNF: Exponential
Probability Model for fault location: Uniform
Total connected load:695.23MW Total connected customer:1675
Reclosers: 23-35, 63-76, 95-102
Sectionalizing switches: 10-11, 10-22, 38-46, 48-61, 78-89, 90-91, 90-119, 103-105, 107-108

A flow chart for the Monte Carlo simulation is shown in Figure 14.

- The simulation starts with generating random numbers for the hours of normal weather and adverse weather in a year, assuming the system is in a normal status at the beginning;
- Time to next fault and the type of fault are then generated according to the current weather condition;
- Location of the fault and time for repairing it is generated next according to the type of fault;
- Results from fault location is then retrieved from database and used in the fault management functions;
- Time consumed in each of the fault management functions is then calculated, and together with time for repair the faulted component, the durations of outage experienced by customers at different part of the system are calculated;

- The simulation then resumes the steps for the next fault;
- At the end of the year, SAIDI and ASIDI is calculated;
- When the means of the yearly values of SAIDI and ASIDI converge, the simulation stops and the cost of outage is calculated using the SAIDI and ASIDI mean values;
- To assess the benefit from the optimization of fault management functions, both fault management before and after optimization are simulated, and the difference in the costs is taken as profit.

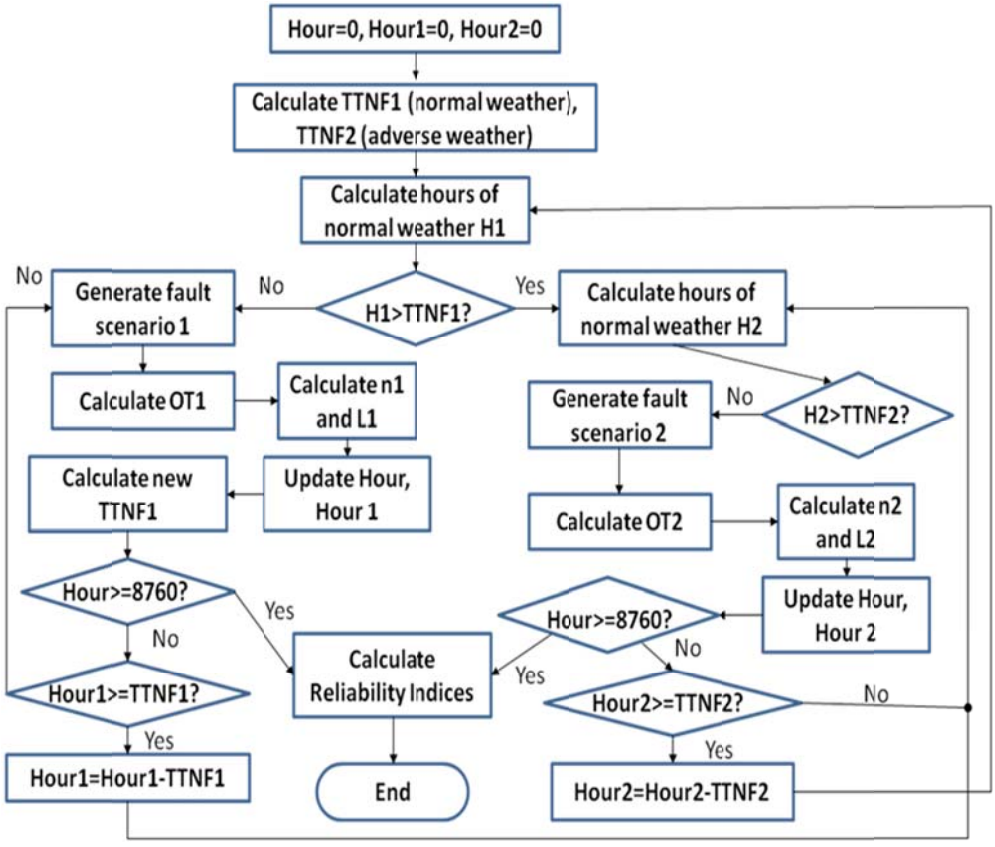

Figure 14 Computation of reliability indices using Monte Carlo simulation

9.4 Conclusion

This section describes the setup for case studies. The simulation is implemented with the hybrid programming in ATP and MATLAB. System model is built in ATP, with interface with MATLAB for generating different fault scenarios; fault location, optimization of crew dispatch and service restoration is programed in MATLAB; the stochastic process for assessment of benefits is also established in MATLAB.

10. CASE STUDY*

10.1 Improved fault location

10.1.1 Overview of case studies

To examine the performance of the proposed method, 1197 fault scenarios and corresponding measurements have been generated as the test cases. None of these scenarios were used during the DT training phase. The generated fault scenarios belong to three categories, and each category consists of three groups. In each group 133 fault scenarios corresponding to the faults happening at node 2 to 134 were simulated. The detailed description of each scenario group is provided in Table 2.

Table 2 Description of Scenario Groups and Rate of Successful Segment Identification

Scenario Group	**Description**	**Accuracy of Segment Identification (%)**
1	R_f=0Ω, no measurement error	**100**
2	R_f=1Ω, no measurement error	**98.5**
3	R_f=5Ω, no measurement error	**100**
4	R_f=0Ω, σ(error)=0.5%	**94.7**
5	R_f=1Ω, σ(error)=0.5%	**92.5**
6	R_f=5Ω, σ(error)=0.5%	**91.7**
7	R_f=1Ω, load at node 21 - 60 increased by 100%	**98.4**
8	R_f=1Ω, load at node 21 - 60 decreased by 50%	**100**
9	R_f=1Ω, load power factor at node 21 - 60 shifted from 0.92 to 0.85	**95.5**

* Part of this chapter is reprinted with permission from "Enhancing Accuracy While Reducing Computation for Voltage-Sag Based Distribution Fault Location" by Y. Dong, C. Zheng and M. Kezunovic, April 2013. *IEEE Trans. Power* Delivery, vol.28, pp.1202-1212, ©2012 IEEE, with permission from IEEE.

10.1.2 Performance of the DT-based segment identifier

With the offline training described in Section 9.2.2, the success rates of the DT-based segment identification are also reported in Table 2. An initial observation of test results reveals that the segment identifier is capable of maintaining a success rate of above 98.5% in all three scenario groups for category one, where no measurement errors were added. For category two in which the measurement errors were considered, the prediction accuracy reduced a little bit, and accuracy greater than 91% were reached for all three groups. In category three, the loads from node 21 to node 60 were varied and the DT performance was tested. As shown in the table, identification accuracy higher than 95.5% was achieved for each group.

10.1.3 Performance under perfect condition

Scenario Groups 1 to 3 are used for tests under "perfect condition". The load information given to the fault location program is consistent with the settings of load impedances in ATP and the measurement values are considered accurate (no errors are added to the phasors and voltage sags). Under such condition the error in fault location comes from the simplification of line model (shunt capacitor being neglected) and computation error.

10.1.4 Comparison before introducing segment identification

Figure 15 shows the comparison of the method from [27] and the proposed node selection method (without segment identification) for Scenario Group 2. The x axis shows the faulted node number, and the y axis is the output error represented by the

distance between calculated and actual location of faults in km. The dotted curve is the error from Pereira's method, and the solid one is the error from the proposed method in Section 5.5.3.

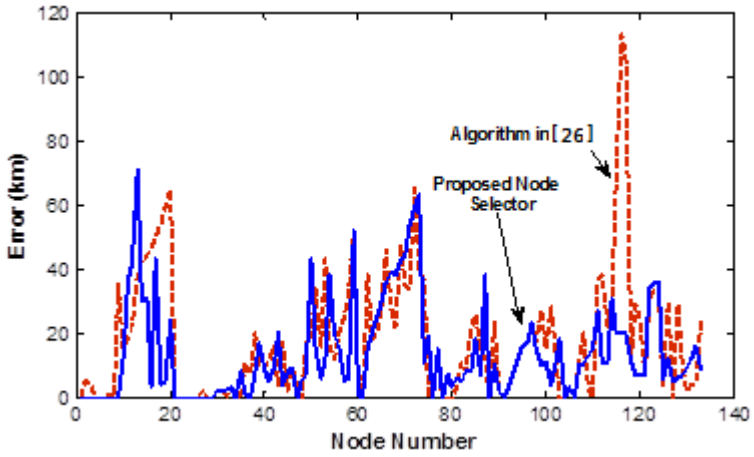

Figure 15 Fault location errors in km with faults along the feeder

On average the proposed node selector reduces the errors by 34.1%. The Mean of errors with faults on the feeder main section has dropped from 15.28 km to 6.15 km, which is less than the average distance between two neighboring nodes. Although in general both methods show better performance with faults on the main section of feeder, the performance goes down as faults occur on nodes towards the end of laterals, for example node 14 and 75. At node 116, Pereira's method selected node 127, causing the error to be higher than 110km, but the proposed method avoided this error.

The main window in Figure 16 illustrated a successful node selection for one of the test fault scenarios. The smallest mismatch is observed at node 24, which is indeed the actual location of fault.

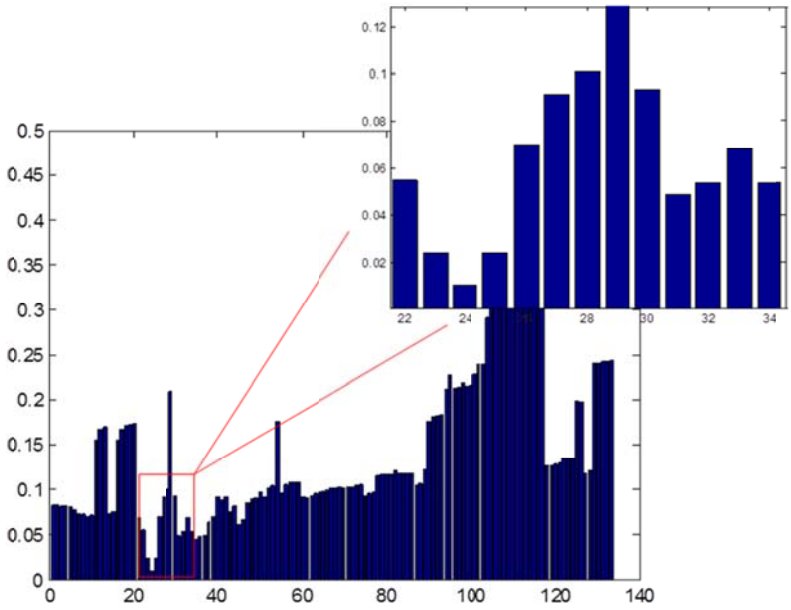

Figure 16 Mismatch calculated for fault at node 24, R_f=0

10.1.5Further improvement with segment identification

Figure 17 shows the outputs from segment identifier with faults at node 2 to 134, Rf=1Ω. The solid line is the actual segment number, and the dashed one shows segment number identified by the decision tree. In this group of fault scenarios node 63 and 75 are misclassified.

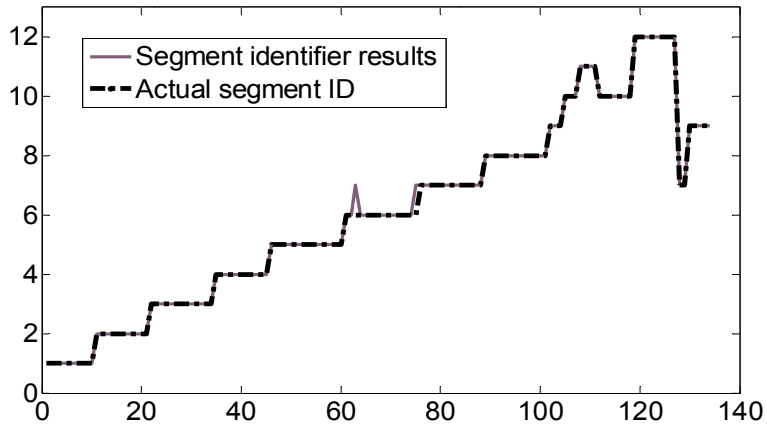

Figure 17 Output from segment identifier, with R_f=1Ω

Figure 18 shows the reduction of error by introducing segment identifier. The dotted line represents errors from method using node selector only (solid line in Figure 15) and the solid line shows errors after utilizing segment identifier. Segment IDs from decision tree has a success rate of 100% for 0Ω faults, 98.5% for 1Ω faults, and 100% for 5Ω faults. It can be seen that spikes at node 74, 87, 101 and some other nodes have been alleviated because the node outside the selected segment has been removed from the list of tentative nodes. However error at node 75 did go up because the node has been misclassified into Segment 7.

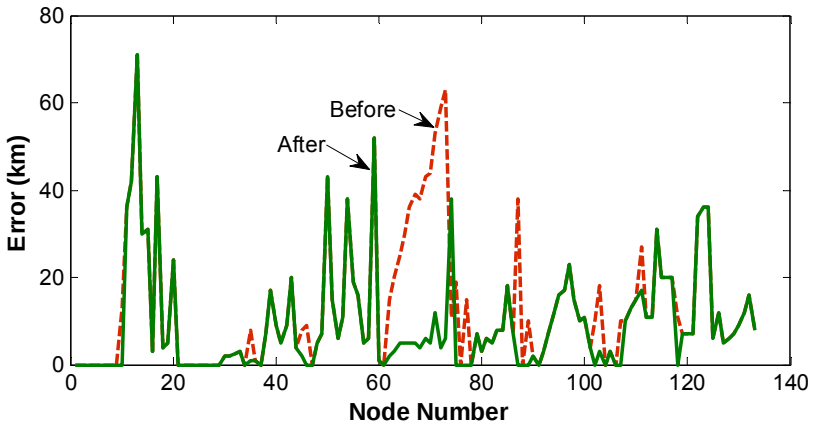

Figure 18 Improvement with segment identifier

In the meantime the computational burden is reduced significantly. For example, both methods are able to successfully locate fault at node 24 (Figure 16). Instead of running load flow for fault being at node 2 to 134, the proposed method takes nodes 22 to 34 as tentative nodes and performs load flow calculation, which reduced the computation by nearly 90%. This means only the nodes in the zoom-in window of Figure 16 were investigated in the proposed algorithm.

10.1.6 Impact of fault resistance

The mean of errors from different settings of fault resistance are recorded in Table 3. “Main”, “L1”, “L2” refers to scenarios with fault on main section, 1st category laterals and 2nd category laterals respectively; “Alg1” and “Alg2” represent algorithm from [27] and the one proposed in this paper respectively. The comparison clearly reveals better performance of the proposed algorithm. Although theoretically the proposed method should not be affected by fault resistance, the test results show otherwise. The accuracy from node selector gradually decreases as the fault resistance goes up. This is because when fault resistance is high, the differences between voltage sags are reduced, and their dominance over the calculated mismatch is compromised by computational errors. Nevertheless the proposed algorithm constantly produces superior results and shows a slower deterioration of accuracy over increasing fault resistance.

Table 3 Errors in Perfect Condition

Rf (Ω)	**Total**		**Main**		**L1**		**L2**	
	Alg1	**Alg2**	**Alg1**	**Alg2**	**Alg1**	**Alg2**	**Alg1**	**Alg2**
0	17.8	11.1	13.6	7.10	17.4	13.4	21.5	12.3
1	18.2	9.49	15.3	3.68	19.6	13.6	19.3	10.6
5	24.7	17.3	20.3	8.90	29.3	19.7	24.3	21.9

10.1.7 Performance under non-perfect condition

The impact of measurement error and inconsistent load condition are evaluated in the test of non-perfect condition (Scenario Group 4 to 9).

Impact of Measurement Error

Scenario Groups 4 to 6 are designed to evaluate the impact of measurement error. Random values of error with mean of 0 and deviation of 0.5% of rated voltage are added to the measurements. Results are recorded in row 1 to 3 of Table 4.

Table 4 Test Results from Non-Perfect Condition Scenarios

Scn.	**Total**		**Main**		**L1**		**L2**	
Grp.	**Alg1**	**Alg2**	**Alg1**	**Alg2**	**Alg1**	**Alg2**	**Alg1**	**Alg2**
4	21.9	11.8	11.4	6.83	24.9	16.0	27.8	12.2
5	26.7	15.4	31.3	5.70	24.7	21.5	24.6	17.8
6	35.6	22.2	27.6	18.5	37.1	22.2	40.7	25.2
7	20.9	12.6	16.6	12.8	25.2	12.9	20.6	12.1
8	18.7	8.73	19.6	3.15	17.6	12.3	19.0	10.2
9	19.9	10.4	15.2	4.5	23.6	15.8	20.4	10.5

Impact of Load Condition

Scenarios for evaluating the impact of load condition is generated by varying the load impedance in ATP model, without updating the load profile used by fault location program. Loads are varied as described in Table 2, Scenario Group 7 to 9. Fault resistance is set as 1Ω. Results are recorded in row 4 to 6 of Table 4. The histogram of the proportions of errors to the distances of actual location from feeder root for fault scenarios in Scenario Group 8 is shown in Figure 19. Most results from the proposed

algorithm contain error of lower than 10% of the distance-to-fault, while Pereira's algorithm produce more results with larger errors.

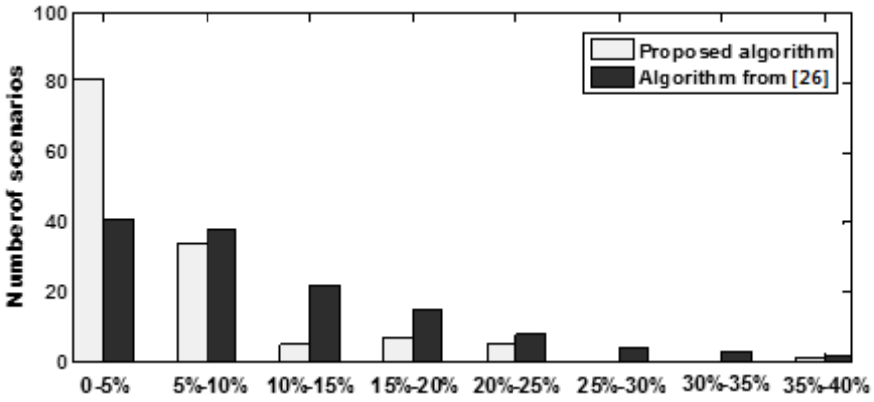

Figure 19 Errors under load variation (Scenario Group 8)

Figure 20 shows the percentage of reduced errors from 9 scenario groups. Generally the errors with faults on the main section of feeder are reduced most significantly, with the highest of over 80%. In every scenario group the mean error for each line type has been reduced.

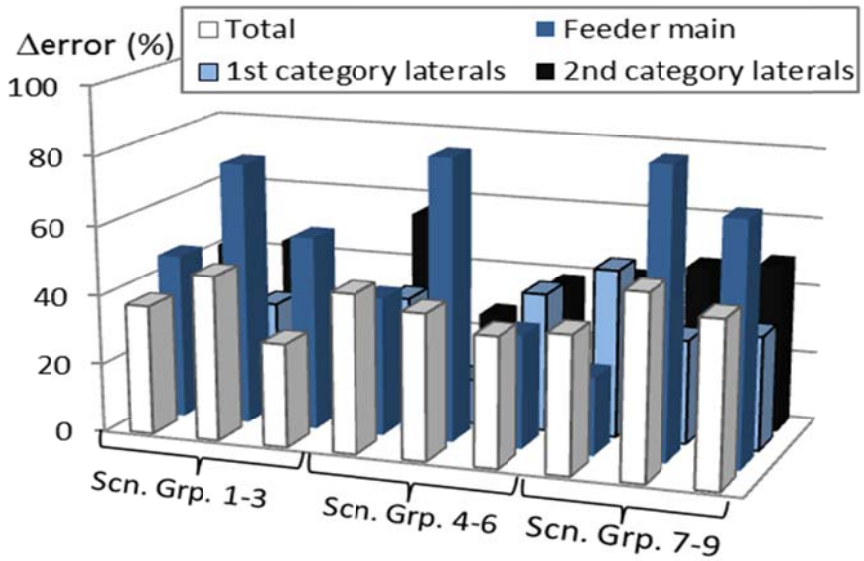

Figure 20 Reduction in fault location errors

10.1.8 Conclusion from case study of fault location

The proposed method has been implemented on an actual distribution system. Experimental analysis indicates a better performance of fault location accuracy and reliability;

The algorithm has been tested extensively under different simulation scenarios. The results show that the proposed method is able to handle certain degree of measurement error and load variations.

10.2 Optimized fault management functions

The voltage sag based fault location produces a list of nodes starting with the most suspected node based on the calculated flag values. Based on the sensitivity study, when data condition is not satisfactory, the true faulted node may not have the largest flag value, but will not fall out of the top few nodes on the list.

10.2.1 Crew dispatch

Once results were obtained from fault location software, optimization process described in Section 6 is implemented to generate work order for the crew to perform field inspection and switching for isolation. The first step is to take the top ten nodes from the list and group them based on the topology of the system. The second step is to determine if any group of nodes can be eliminated by isolation attempts (switching operation). If there are still multiple groups (nodes on different laterals) then generate the optimal inspection sequence using (3). Probabilities from (3) are calculated by the ranking of nodes.

Four cases are generated to demonstrate the procedures, with artificially created node numbers:

1) Suspected nodes: 15, 16, 17, 18, 12, 13, 14, 19, 20, 21, forming two areas but under one switch.

2) Suspected nodes: 112, 113, 108, 106, 109, 105, 114, 115, 116, 127, forming two areas in series and one separated area (127); recloser lock-out at 96.

3) Suspected nodes: 91, 119, 120, 92, 122, 93, 121, 94, 123, 125, forming two areas under two switches;

4) Suspected nodes: 79, 84, 80, 85, 81, 86, 81, 128, 83, 86, forming two geographical areas under one fuse.

The total number of available crew is 2. The optimal plan for fault location and isolation are recorded in Table 5.

Table 5 Optimized Fault Location and Isolation Plan

Case NO.	Switching plan	Inspection plan
1	None	Go to Node 11 and search the area behind blown fuse
2	Open S103-105; Close R95-102	Go to Node 112 and search downstream; If fault is not found, search from 106 and go upstream
3	Open S90-91, close R63-76; If unsuccessful, Open S90 -119 and close R63-76	Go to the disconnected area

Table 5 Continued

Case NO.	Switching plan	Inspection plan
4	None	Send one crew to each area

10.2.2 System reconfiguration

The connectivity to adjacent feeders is listed in Table 6. Three reconfiguration strategies are analyzed and compared:

1) RecS1: whenever the connectivity allows;

2) RecS2: whenever fault occurs on the main section of feeder and before R63-76;

3) RecS3: whenever fault occurs on the main section of feeder and before R23-35.

The calculated Risk for RecS1-RecS3 from Monte Carlo simulation is shown in Figure 21, with time for switching varies from 15 minutes to 1.5 hours. When average T_{SWC} is less than 30 minutes RecS1 produces the lowest Risk; when average T_{SWC} exceeds 45 minutes Risk of RecS3 becomes the lowest among the three. The result shows that when time for switching is very short, for example with distribution automation devices, post-fault reconfiguration should be deployed whenever is feasible. However if switching is done manually and takes a relatively long time, the reconfiguration should be deployed only when a large portion of load is disconnected.

10.3 Assessment of benefit

10.3.1 Reliability before optimization

As mentioned in [42], the reliability indices in 100 years are calculated in each iteration of the Monte Carlo simulation. Simulation stops when change in average values of SAIDI and ASIDI are less than 0.001. Target SAIDI is set as 60% of the original SAIDI.

Table 6 Connectivity to Adjacent Feeders

Adjacent Feeder	Connected-to-Node	Capacity (MW)
2	51	70
3	127	28
3	129	90
4	14	80
5	75	90
6	103	53
7	118	38
8	111	34

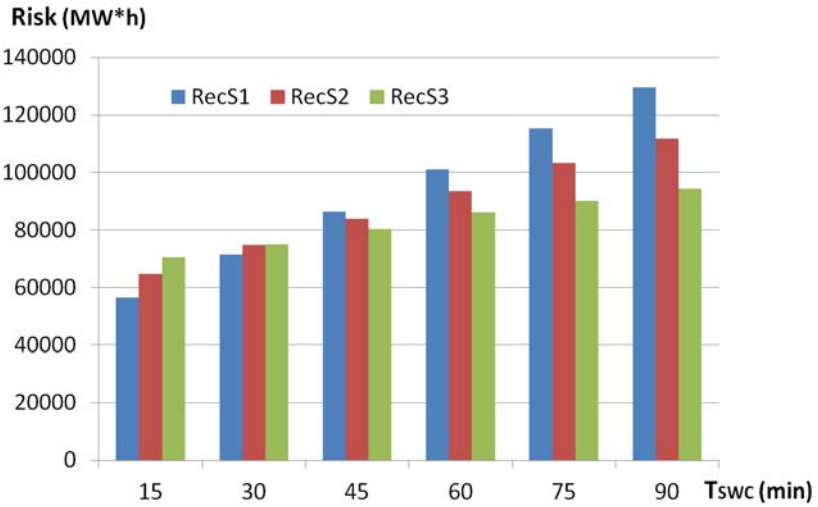

Figure 21 ASIDIs calculated with different T_{SWC}

Without information of location of utility maintenance office, travel time is set as proportional to the distance of substation to the fault's immediate upstream switching equipment. In the original status (before optimization), time for locating the fault is proportional to distance of the immediate upstream switching devices to faulted point. Figure 22 shows values of SAIDI from Monte Carlo simulation for original status (without optimization). Figure 22 (a) is the ascending sorted results, and Figure 22 (b) is the histogram. Average SAIDI is 140.5 min/customer/year, resulting in the target SAIDI as 84.28.

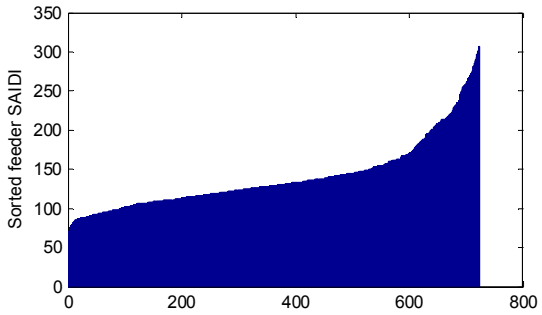

(a) Sorted SAIDI results

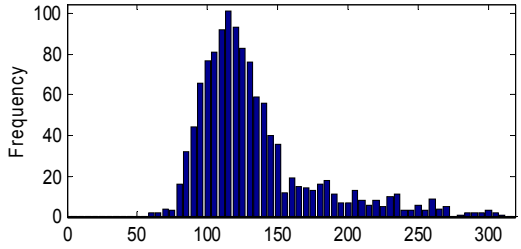

(b) Histogram of SAIDI

Figure 22 SAIDI results for original status

10.3.2 Impact of optimized fault location and isolation

After the optimization of fault location and isolation, travel time becomes proportional to distance between substation and calculated location of fault. Time for

inspection becomes proportional to the error of fault location computation. Mean and variance of SAIDI and ASIDI, and the associated cost are recorded in **Table 7**, in the row of OFL (optimized fault location). After optimization of fault location and isolation the average value of SAIDI value drops to lower than the target SAIDI value, meaning the criterion for improvement in reliability has been met.

10.3.3Impact of reconfiguration strategies

Since target SAIDI has been met, SAIDI is no longer a target of interest. ASIDI for the three reconfiguration strategies is also recorded in **Table 7**, in the row of RecS1-RecS3. Feeder automation devices are assumed available. Time for computing reconfiguration schedule (T_{COM}) is set as 30 minutes, and time for switching (T_{SWC}) is proportional to the number of switching operations. To simplify computation only capacity constraint is considered when planning for a reconfiguration. It is worth noticing that reconfiguration has a significant effect of reducing both mean and variance of the indices. Figure 23 shows comparison of the sorted ASIDI calculated for RecS1 (blue) with original ASIDI (red), with number of Monte Carlo simulation iterations scaled to 1. It can be seen that the large ASIDI values at the tail have disappeared, indicating the severity of large-scale faults has been alleviated by connecting customers to alternative power supply routes.

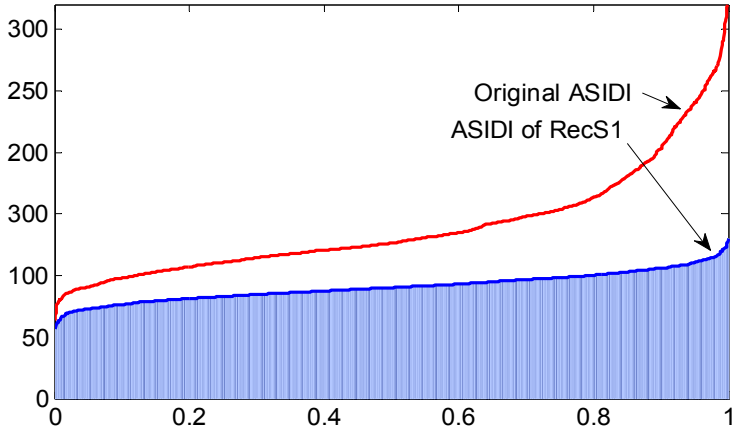

Figure 23 ASIDIs of RecS1, T_{COM}=30 min

Table 7 Simulation Results

Scenario	SAIDI		ASIDI		Loss $	Profit ($ *ΔLoss*)
	Mean	Var	Mean	Var		
Original	140.5	1991	141.2	2029	146572	-----
OFL	117.8	1186	135.5	1390	134963	11610
RecS1	66.62	93.95	81.27	111.7	75335	71237
RecS2	84.83	81.73	93.53	104.1	86853	59718
RecS3	96.28	101.2	100.8	116.8	96789	49783

The assessment of benefit clearly shows how the reliability got improved through optimization of fault management tasks. On the one hand, both mean and variance of individual reliability indices of SAIDI and ASIDI are reduced, indicating customers are experiencing shorter outages and more stable power supply over the years. One the other hand, analysis of cost shows that utilities are rewarded by considerable profits from improving their response to faults every year.

10.4 Conclusion

- Utilization of additional data from the system IEDs improves the performance of fault location, and fault management tasks that follow;
- Time delay in processing the fault scenario caused by lack of fault information can be significantly reduced by implementing feeder automation techniques and risk-based analysis;
- Simulation of different reconfiguration strategies shows that with remote-controlled switches a more effective system reconfiguration is possible;
- Impact of fault management automation and optimization is assessed through Monte Carlo simulation, and the results show quantified improvement in system reliability both in values of the reliability indices and associated cost;
- Besides the improvement in the average of system reliability, Monte Carlo simulation also reveals a reduced fluctuation in reliability over the years.

11. CONCLUSION

11.1 Research achievements and contributions

In this research, improvement in system reliability through optimized fault location and fault management tasks is studied and validated. The main achievements of the research include:

- The cost associated with outages is formulated quantitatively, based on research of utility's loss and customer's willingness for better system reliability
- The impact of fault management on system reliability is established through outage cost
- Improved fault location method is proposed, using data from IEDs installed in the system
- The utilization of fault location results on man-involved fault management functions is discussed, and the optimization of such fault management functions is proposed
- The proposed fault location method and optimization of fault management functions are implemented on a real distribution system
- The benefit on system reliability from the proposed fault location method and the optimized fault management is assessed through Monte Carlo simulation of outages

11.2 Conclusions

Following has been concluded from the case studies:

- Utilization of additional data from the system IEDs improves the performance of fault location, and fault management functions that follow
- The proposed fault location methods shows better performance, both in accuracy and in robustness to input errors and other unpredicted conditions
- Time delay in processing the fault scenario caused by lack of fault information can be significantly reduced by implementing feeder automation techniques and risk-based analysis
- Simulation of different reconfiguration strategies shows that with remote-controlled switches a more effective system reconfiguration is possible
- Impact of fault management automation and optimization is assessed through Monte Carlo simulation, and the results show quantified improvement in system reliability both in values of the reliability indices and associated cost
- Besides the improvement in the average of system reliability, Monte Carlo simulation also reveals a reduced fluctuation in reliability over the years

11.3 Suggestions for future work

- The number of measurements and the location of the sensors are two important issues that affect the accuracy of the proposed fault location algorithm. Future work should include the optimization of sensor number/placement.

- Customers' willingness to pay for better service may vary according to the quality of service they already have. Typically when an outage last longer, the price customers are willing to pay for extra energy per kWh is higher. In the future work, a changing rate on undelivered power should be considered for formulating the outage cost.
- Currently the optimization problem is solved heuristically. Approach for solving nonlinear and/or integral optimization problems should be studied for the optimization of fault management tasks.
- A distribution system with certain penetration of DGs and loop topologies should be considered for future case study, to provide more convincing results, though theoretically the proposed approaches shouldn't be affected by the connectivity and operating conditions of the system.

REFERENCES

[1] R.E. Brown, A.P. Hanson, H.L. Willis, F.A. Luedtke and M.F. Born," Assessing the reliability of distribution systems," Computer Applications in Power, vol.14, no. 1, pp.44-49, January 2001.

[2] M. Y. Chow, L. S. Taylor, and M. S. Chow, "Time of outage restoration analysis in distribution systems," IEEE Trans. Power Del., vol.11, no.3, pp.1652-1658, July 1996.

[3] R. Horn and P. Johnson, "Outage management applications and methods panel session: outage management techniques and experience," IEEE Power Engineering Society 1999 Winter Meeting, vol.2, pp. 866- 869, February 1999.

[4] K. Sridharan and N. N. Schulz, "Outage management through AMR systems using an intelligent data filter," IEEE Trans. Power Del., vol.16, no.4, pp.669-675, October 2001.

[5] T. Gonen, “Electric power distribution system engineering”, New York: McGraw-Hill, 1986.

[6] Lawrence Berkley National Laboratory, "Examination of Temporal Trends in Electricity Reliability Based on Reports from U.S. Electric Utilities, " Lawrence Berkley National Laboratory report, No. LBNL-5268E, January 2012 [Online]. Available: http://certs.lbl.gov/pdf/lbnl-5268e.pdf.

[7] M. Kezunovic, "Smart Fault Location for Smart Grids," IEEE Trans. Smart Grid, vol. 2, no. 1, pp 11-22, March 2011.

[8] C. Zheng and M. Kezunovic, "Impact of Wind Generation Uncertainty on Power System Small Disturbance Voltage Stability: A PCM-based Approach," Electric Power Systems Research Journal, Vol. 84, No. 1, pp 10-19, March 2012.

[9] C. Zheng, Y. Dong, O. Gonen, and M. Kezunovic "Data Integration Used in New Applications and Control Center Visualization Tools," IEEE PES General Meeting, Minneapolis, USA, July 2010.

[10] Roy Hoffman, "Automated Distribution Feeder Fault Management: Possibilities and Challenges," Electric Energy T&D Magazine, pp. 44-47, July/August 2009.

[11] CIRED Working Group WG03 Fault Management, "Fault management in electrical distribution system," final report of CIRED WG03, December 1998.

[12] A. Pahwa, "Role of distribution automation in restoration of distribution systems after emergencies," IEEE Transmission and Distribution Conference and Exposition, Oct. 2001.

[13] IEEE guide for electric power distribution reliability indices, IEEE Std. 1366-2003, May 2004.

[14] E. Fumagalli and L. Schiavo, "Regulating and Improving the Quality of Electricity Supply: the Case of Italy", European Review of Energy Markets, vol. 3, no. 3, Oct. 2009.

[15] S. T. Mak, "A synergistic approach to using AMR and intelligent electronic devices to determine outages in a distribution network," Power Systems Conference, Clemson, 2006.

[16] K. Sridharan and N. N. Schulz, "Outage management through AMR systems using an intelligent data filter," IEEE Trans. Power Del., vol.16, no.4, pp.669-675, October 2001.

[17] A. A. Girgis, C. M. Fallon, and D. L. Lubkeman, "A Fault Location Technique for Rural Distribution Feeders," IEEE Trans. Industry App., vol. 29, no. 6, pp. 1170-1175, December 1993.

[18] R. Das, "Determining the locations of faults in distribution systems", Ph.D. dissertation, Saskatchewan Univ., Canada, 1998

[19] L. Yuan, "Generalized Fault-Location Methods for Overhead Electric Distribution Systems," IEEE Trans. Power Del., vol. 26, no. 1, pp.53-64, January 2011.

[20] S. Das, N. Karnik and S. Santoso, "Distribution Fault-Locating Algorithms Using Current Only," IEEE Trans. Power Del., vol. 27, no. 3, pp.1144-1153, July 2012.

[21] R.H. Salim, M. Resener, A.D. Filomena, K. Rezende Caino de Oliveira and A.S. Bretas, "Extended Fault-Location Formulation for Power Distribution Systems," IEEE Trans. Power Del., vol. 24, no. 2, pp.508-516, April 2009.

[22] M. S. Choi, S. J. Lee, D. S. Lee, and B. G. Jin, "A new fault location algorithm using direct circuit analysis for distribution systems," IEEE Trans. Power Del., vol. 19, no. 1, pp. 35-41, January 2004.

[23] A. Borghetti, M. Bosetti, C.A. Nucci, M. Paolone, and A. Abur, "Integrated Use of Time-Frequency Wavelet Decompositions for Fault Location in Distribution Networks: Theory and Experimental Validation," IEEE Trans. Power Del., vol. 25, no. 4, pp. 3139-3146, October 2010.

[24] A. Borghetti, M. Bosetti, M. Di Silvestro, C. A. Nucci, and M. Paolone, "Continuous-wavelet transform for fault location in distribution power networks: Definition of mother wavelets inferred from fault originated transients," IEEE Trans. Power Syst., vol. 23, no. 2, pp. 380–388, May 2008.

[25] F. H. Magnago and A. Abur, "Fault location using wavelets," IEEE Trans. Power Del., vol. 13, no. 4, pp. 1475–1480, October 1998.

[26] Z. Galijasevic and A. Abur, "Fault location using voltage measurements," IEEE Trans. Power Del., vol. 17, no. 2, pp. 441-445, April 2001.

[27] R. A. F. Pereira, L. G. W. Silva, M. Kezunovic, and J. R. S. Mantovani "Improved fault location on distribution feeders based on matching during-fault voltage sags," IEEE Trans. Power Del., vol. 24, no. 2, pp. 852-862, April 2009.

[28] S. Lotfifard, M. Kezunovic, M.J. Mousavi, "Voltage Sag Data Utilization for Distribution Fault Location," IEEE Trans. Power Del., vol. 26, no. 2, pp 1239-1246, April 2011.

[29] P. M. S. Carvalho, F. J. D. Carvalho, and L. A. F. Ferreira, "Dynamic Restoration of Large-Scale Distribution Network Contingencies: Crew Dispatch Assessment," IEEE PowerTech, Lausanne, July 2007.

[30] S. Toune, H. Fudo, T. Genji, Y. Fukuyama, and Y. Nakanishi, "Comparative Study of Modern Heuristic Algorithms to Service Restoration in Distribution Systems," IEEE Trans. Power Del., vol. 17, no. 1, pp. 173-181, Jan. 2002.

[31] M. W. Siti, D. V. Nicolae, A. A. Jimoh, and A. Ukil, "Reconfiguration and Load Balancing in the LV and MV Distribution Networks for Optimal Performance," IEEE Trans. Power Del., vol.22, no.4, pp.2534-2540, Oct. 2007.

[32] C. C. Liu, S. J. Lee, and K. Vu, "Loss minimization of distribution feeders: Optimality and algorithms," IEEE Trans. Power Del., vol. 4, no. 2, pp. 1281–1289, April 1989.

[33] C. S. Cheng and D. Shirmohammadi, "A three-phase power flow method for real-time distribution system analysis," IEEE Trans. Power Syst., vol. 10, no. 2, pp. 671-679, May 1995.

[34] Steinberg, Dan and Mikhail Golovnya, CART 6.0 User's Manual. San Diego, CA: Salford Systems, 2006.

[35] L. Breiman, J. Friedman, R. A. Olshen, and C. J. Stone, Classification and Regression Trees. Pacific Grove: Wadsworth, 1984.

[36] C. Zheng, V. Malbasa, and M. Kezunovic, "A Fast Stability Analysis Scheme based on Classification and Regression Tree," IEEE Conference on Power System Technology (POWERCON), Auckland, New Zealand, October 2012.

[37] Y. Dong, V. Aravinthan, M. Kezunovic, and W. Jewell, "Integration of asset and outage management tasks for distribution systems," IEEE Power & Energy Society 2009 General Meeting, pp.1-8, July 2009.

[38] Luis G. Wesz da Silva, Rodrigo A. Fernandes Pereira, Juan Rivier Abbad, José R. Sanches Mantovani, "Optimised placement of control and protective devices in

electric distribution systems through reactive tabu search algorithm," Electric Power Systems Research, Volume 78, Issue 3, pp. 372-381, March 2008.

[39] Electrical Energy Systems Planning Laboratory Practical 135 Bus Feeder Data. Available: http://www.dee.feis.unesp.br/lapsee/TestSystems/135_Bus_Feeder.pdf.

[40] C. Zheng and M. Kezunovic, "Impact of Grid Connected Doubly Fed Induction Wind Generators on Voltage Stability," IEEE PowerTech 2011, Trondheim, June 2011.

[41] C. Zheng and M. Kezunovic "Distribution System Voltage Stability Analysis with Wind Farms Integration," IEEE PES 42nd North American Power Symposium (NAPS), Arlington, USA, September, 2010.

[42] N. Balijepalli, S. S. Venkata, and R. D. Christie, "Modeling and analysis of distribution reliability indices," IEEE Trans. Power Del., vol.19, no.4, pp. 1950-1955, Oct. 2004.

APPENDIX

DATA SHEET OF THE 134-NODE DISTRIBUTION SYSTEM

The test system is a typical 13.8 kV, 134-node, overhead three-wire distribution feeder that has reconfiguration possibility with other seven neighboring feeders. This feeder has been used by researchers from Electrical Energy Systems Planning Laboratory at UNESP – Ilha Solteira, Brazil to carry out studies and analyses of techniques and algorithms related to electric power distribution problems, such as supplying reliability, optimal placement of protective and control devices, and fault location [34], [39].

If not otherwise specified, the load power factor is 0.92. The line sections, length of sections, conductor size and load connected at receiving node of each line section is recorded in Table A-1. The line impedance matrices for each conductor size are presented following Table A-1.

Table A- 1 Line sections, length of sections, conductor size and load connected at receiving node of each line section

Sending Node	Receiving Node	Length (m)	Conductor Type	Load (KVA)
0	1			
1	2	900,00	#4/0	0,00
2	3	50,00	#2	45,00
2	4	100,00	#4/0	0,00
4	5	40,00	#4/0	75,00
5	6	200,00	#4/0	75,00
6	7	200,00	#4/0	112,50
7	8	200,00	#4/0	75,00

Table A-1 Continued

Sending Node	Receiving Node	Length (m)	Conductor Type	Load (KVA)
8	9	10,00	#4/0	75,00
9	10	50,00	#4/0	0,00
10	11	100,00	#4	0,00
11	12	60,00	#4	8,60
12	13	30,00	#4	75,00
13	14	160,00	#4	75,00
11	15	30,00	#4	112,50
15	16	10,00	#4	45,00
16	17	20,00	#4	112,50
17	18	40,00	#4	0,00
18	19	40,00	#2	75,00
19	20	50,00	#2	112,50
18	21	150,00	#2	112,50
10	22	30,00	#4/0	112,50
22	23	70,00	#4/0	0,00
23	24	50,00	#4	3,00
24	25	20,00	#4	45,00
25	26	30,00	#4	0,00
26	27	60,00	#2	112,50
27	28	40,00	#2	0,00
28	29	20,00	#2	75,00
29	30	120,00	#2	112,50
28	31	20,00	#2	112,50
26	32	20,00	#4	112,50
32	33	5,00	#4	112,50
33	34	25,00	#4	112,50

Table A-1 Continued

Sending Node	Receiving Node	Length (m)	Conductor Type	Load (KVA)
35	36	70,00	#4/0	12,40
36	37	10,00	#4/0	112,50
37	38	10,00	#4/0	0,00
38	39	70,00	#4/0	3,00
38	40	100,00	#4/0	0,00
40	41	60,00	#4	75,00
40	42	50,00	#4	75,00
42	43	10,00	#4	75,00
40	44	30,00	#4/0	112,50
44	45	40,00	#4/0	45,00
38	46	60,00	#4/0	1,00
46	47	20,00	#4/0	112,50
47	48	120,00	#4/0	0,00
48	49	50,00	#4/0	112,50
49	50	20,00	#4/0	75,00
50	51	170,00	#4/0	112,50
48	52	100,00	#4/0	0,00
52	53	60,00	#4	1,20
53	54	30,00	#4	112,50
54	55	130,00	#4	75,00
52	56	20,00	#4	75,00
56	57	80,00	#4	0,00
57	58	50,00	#2	10,00
57	59	60,00	#2	112,50
59	60	20,00	#2	3,80
48	61	40,00	#4/0	3,00

Table A-1 Continued

Sending Node	Receiving Node	Length (m)	Conductor Type	Load (KVA)
62	63	50,00	#4/0	0,00
63	64	30,00	#1/0	75,00
64	65	20,00	#1/0	75,00
65	66	30,00	#1/0	3,50
66	67	20,00	#1/0	0,00
67	68	30,00	#4	112,50
67	69	20,00	#4	7,00
69	70	20,00	#4	112,50
67	71	50,00	#1/0	75,00
71	72	40,00	#1/0	8,50
72	73	40,00	#1/0	1,90
73	74	20,00	#1/0	112,50
74	75	110,00	#1/0	112,50
63	76	20,00	#4/0	112,50
76	77	30,00	#4/0	5,90
77	78	50,00	#4/0	0,00
78	79	70,00	#4/0	75,00
79	80	70,00	#4/0	112,50
80	81	30,00	#4/0	112,50
81	82	30,00	#4/0	0,00
82	83	50,00	#4	75,00
82	84	50,00	#4/0	75,00
84	85	30,00	#4/0	112,50
85	128	20,00	#4/0	0,00
128	86	30,00	#4/0	15,50
86	87	20,00	#4/0	75,00

Table A-1 Continued

Sending Node	Receiving Node	Length (m)	Conductor Type	Load (KVA)
78	89	50,00	#4/0	75,00
89	90	50,00	#4/0	0,00
90	91	180,00	#4/0	45,00
91	92	20,00	#4/0	0,00
92	93	30,00	#2	112,50
92	94	70,00	#2	23,50
92	95	100,00	#4/0	0,00
95	96	40,00	#2	75,00
95	97	50,00	#2	6,00
97	98	60,00	#2	0,00
98	99	110,00	#4	23,50
98	100	40,00	#2	75,00
100	101	110,00	#2	112,50
95	102	60,00	#4/0	112,50
102	103	40,00	#4/0	0,00
103	104	30,00	#1/0	75,00
103	105	150,00	#1/0	75,00
105	106	210,00	#1/0	108,50
106	107	30,00	#1/0	0,00
107	108	100,00	#1/0	0,00
108	109	100,00	#4	108,50
109	110	30,00	#4	112,50
110	111	20,00	#4	112,50
107	112	170,00	#4/0	75,00
112	113	110,00	#4/0	0,00
113	114	110,00	#4	0,00

Table A-1 Continued

Sending Node	Receiving Node	Length (m)	Conductor Type	Load (KVA)
115	116	200,00	#4	30,00
116	117	200,00	#4	30,00
117	118	200,00	#4	30,00
90	119	110,00	#2	0,00
119	120	70,00	#4/0	0,00
120	121	70,00	#4/0	30,00
119	122	70,00	#2	55,00
122	123	130,00	#4	0,00
123	124	20,00	#4	15,50
123	125	20,00	#4	15,50
125	126	40,00	#4	45,00
126	127	40,00	#4	112,50
128	129	60,00	#2	45,00
104	130	70,00	#1/0	0,00
130	131	20,00	#4/0	112,50
130	132	100,00	#1/0	0,00
132	133	40,00	#1/0	112,50
133	134	40,00	#1/0	112,50

Shunt admittances are neglected and network line impedance matrices are defined as follows:

– Section 0 – 1. It is an equivalent impedance matrix corresponding to the impedances of generation, transmission and substation transformer:

$$[Z_{0-1}] = \begin{bmatrix} 0{,}2900 + j1{,}9200 & 0{,}1960 + j0{,}5300 & 0{,}1960 + j0{,}5300 \\ 0{,}1960 + j0{,}5300 & 0{,}2900 + j1{,}9200 & 0{,}1960 + j0{,}5300 \\ 0{,}1960 + j0{,}5300 & 0{,}1960 + j0{,}5300 & 0{,}2900 + j1{,}9200 \end{bmatrix} \quad [\Omega]$$

– Sections with conductor size #2:

$$[Z_{\#2}] = \begin{bmatrix} 1{,}0840 + j0{,}9980 & 0{,}0600 + j0{,}4780 & 0{,}0600 + j0{,}4500 \\ 0{,}0600 + j0{,}4780 & 1{,}0840 + j0{,}9980 & 0{,}0600 + j0{,}5360 \\ 0{,}0600 + j0{,}4500 & 0{,}0600 + j0{,}5360 & 1{,}0840 + j0{,}9980 \end{bmatrix} \quad [\Omega / Km]$$

– Sections with conductor size #4:

$$[Z_{\#4}] = \begin{bmatrix} 1{,}6440 + j1{,}0060 & 0{,}0600 + j0{,}4780 & 0{,}0600 + j0{,}4500 \\ 0{,}0600 + j0{,}4780 & 1{,}6440 + j1{,}0060 & 0{,}0600 + j0{,}5360 \\ 0{,}0600 + j0{,}4500 & 0{,}0600 + j0{,}5360 & 1{,}6440 + j1{,}0060 \end{bmatrix} \quad [\Omega / Km]$$

– Sections with conductor size #1/0:

$$[Z_{\#1/0}] = \begin{bmatrix} 0{,}7567 + j1{,}0067 & 0{,}0600 + j0{,}4780 & 0{,}0600 + j0{,}4500 \\ 0{,}0600 + j0{,}4780 & 0{,}7567 + j1{,}0067 & 0{,}0600 + j0{,}5360 \\ 0{,}0600 + j0{,}4500 & 0{,}0600 + j0{,}5360 & 0{,}7567 + j1{,}0067 \end{bmatrix} [\Omega / Km]$$

– Sections with conductor size #4/0:

$$[Z_{\#4/0}] = \begin{bmatrix} 0{,}4272 + j0{,}9609 & 0{,}0600 + j0{,}4780 & 0{,}0600 + j0{,}4500 \\ 0{,}0600 + j0{,}4780 & 0{,}4272 + j0{,}9609 & 0{,}0600 + j0{,}5360 \\ 0{,}0600 + j0{,}4500 & 0{,}0600 + j0{,}5360 & 0{,}4272 + j0{,}9609 \end{bmatrix} [\Omega / Km]$$